

TECHNISCHE UNIVERSITÄT MÜNCHEN

Institut für Neurowissenschaften

**Synaptic signaling by mGluR1 and TRPC3 in
spiny dendrites of cerebellar Purkinje cells**

Horst Alfred Henning

Vollständiger Abdruck der von der Fakultät für Medizin der Technischen
Universität München zur Erlangung des akademischen Grades eines

Doctor of Philosophy (Ph.D.)

genehmigten Dissertation.

Vorsitzender: apl. Prof. Dr. Helmuth Karl Heinz Adelsberger

Prüfer der Dissertation:
1. Univ.-Prof. Dr. Arthur Konnerth
2. Priv.-Doz. Dr. Jana Eveline Hartmann

Die Dissertation wurde am 17.03.2011 beim Studienausschuss des Ph.D.
Studiengangs Medical Life Science and Technology an der Fakultät für Medizin
der Technischen Universität München eingereicht und durch die Fakultät für
Medizin am 18.03.2011 angenommen.

Table of contents

Table of contents	I
Glossary	III
1 Introduction	2
1.1 Metabotropic glutamate receptors	2
1.2 Purkinje cells	5
1.3 mGluR1 and cerebellar function	6
1.4 Synaptic transmission at parallel fiber synapses	7
1.5 Transient Receptor Potential Channels in Purkinje cells	10
1.6 Aim of the study	12
2 Materials and Methods	13
2.1 Animals	13
2.2 Solutions and Pharmacology	13
2.3 Brain slice preparation	14
2.4 Electrophysiology	15
2.5 Fluorescence microscopy	16
2.5.1 Spinning disk confocal microscopy	16
2.5.2 AOD - based two photon microscopy	17
2.5.3 Ca^{2+} indicator	19
2.6 Analysis	20
3 Results	22
3.1 mGluR1 – mediated signaling is intact in the absence of TRPC1	22
3.2 The mGluR1 dependent current is abolished in the absence of TRPC3	23
3.3 The Ca^{2+} transient in the absence of TRPC3 is mediated by mGluR1-dependent Ca^{2+} release from internal Ca^{2+} stores	24
3.4 AMPA receptor-mediated EPSCs are normal in the absence of TRPC3	25
3.5 Two synaptic Ca^{2+} signaling components downstream of mGluR1	28

3.6	Two components of agonist-evoked mGluR1-dependent dendritic Ca ²⁺ signals	30
3.7	Synaptic mGluR1-dependent Ca ²⁺ signals in Purkinje cell spines	33
3.8	Quantitative comparison of mGluR1-dependent spine Ca ²⁺ transients evoked by sparse and dense parallel fiber stimulation	36
3.9	Synaptically evoked TRPC3-mediated Ca ²⁺ -influx in spines	38
3.10	Synaptically evoked mGluR1-mediated Ca ²⁺ -release in spines	41
3.11	Contribution of TRPC3 to mGluR1-mediated spine Ca ²⁺ signaling	43
3.12	TRPC3 is not involved in LTD induction	45
3.13	Synaptically evoked mGluR1-dependent Ca ²⁺ release is robust in the absence of TRPC3	47
4	Discussion	49
5	Publications	55
6	Acknowledgements	56
7	References	57

Glossary

ACSF	Artificial cerebrospinal fluid
AMPA	AMPA receptors
AOD	Acousto-optical deflector
AP	Action potential
BDNF	Brain - derived neurotrophic factor
Ca ²⁺	Calcium ions
CF	Climbing fiber
CNS	Central nervous system
CNQX	6-Cyano-7-nitroquinoxaline-2,3-dione disodium
CPA	Cyclo piazonic acid
DAG	Diacylglycerol
DCN	Deep cerebellar nuclei
$\Delta F/F$	Relative fluorescent change
fs	Femto second (10^{-15} s)
DHPG	3,5-Dihydroxyphenylglycine
DPFS	Dense parallel fiber stimulation
EPSC	Excitatory postsynaptic current
ER	Endoplasmatic reticulum
ES	Extracellular solution
fEPSC	Fast excitatory postsynaptic current
GC	Granule cell
GL	Granular layer
InsP ₃	Inositol 1,4,5-trisphosphate
InsP ₃ R	Inositol 1,4,5-trisphosphate receptor
IS	Intracellular solution
ISI	Interstimuls interval
KO	Knock out
K _d	Dissociation constant
LBD	Ligand binding domain
LTD	Long term depression
mGluR	Metabotropic glutamate receptor
mGluR1	Metabotropic glutamate receptor subtype 1

MF	Mossy fiber
ML	Molecular layer
mM	Millimolar (10^{-3} mol)
μm	Micrometer (10^{-6} m)
mW	Milliwatt (10^{-3} W)
Na^+	Sodium ions
NCX	$\text{Na}^+/\text{Ca}^{2+}$ exchanger
nm	Nanometer (10^{-9} m)
OGB1	Oregon Green BAPTA 1
pA	Picoampere (10^{-12} A)
PC	Purkinje cell
PCL	Purkinje cell layer
PF	Parallel fiber
PIP_2	Phosphoinositol 4,5-bisphosphate
$\text{PLC}\beta$	PhospholipaseC β
PPF	Paired pulse facilitation
PPR	Paired-pulse ratio
R_s	Series resistance
ROI	Region of interest
RT-PCR	Reverse transcription polymerase chain reaction
sEPSC	Slow excitatory postsynaptic current
SERCA	Smooth endoplasmatic reticulum Ca^{2+} ATPase
SPFS	Sparse parallel fiber stimulation
TIFF	Tagged image file format
Ti:Sa	Titan:Saphire
TRP	Transient receptor potential channel
VGCC	Voltage gated calcium channels
7TMD	Seven transmembrane domain

1 Introduction

1.1 Metabotropic glutamate receptors

For more than half a century, glutamate is established as the main excitatory neurotransmitter in the central nervous system underlying fast excitatory neurotransmission in the mammalian brain (Curtis et al., 1960; Hayashi, 1952). In the mid 1980s it had been demonstrated, that glutamate is also able to evoke metabolic actions in neurons via receptors coupled to G proteins (Nicoletti et al., 1986a; Nicoletti et al., 1986b; Sladeczek et al., 1985; Sugiyama et al., 1987). These receptors were termed metabotropic glutamate receptors (mGluRs). Today it is widely accepted that glutamate receptors fall into two major classes, the ionotropic glutamate receptors (iGluRs) which are ligand gated cation channels (Dingledine et al., 1999) and the metabotropic glutamate receptors (mGluRs) which by themselves do not form an ion permeable pore, but are coupled to intracellular signaling pathways.

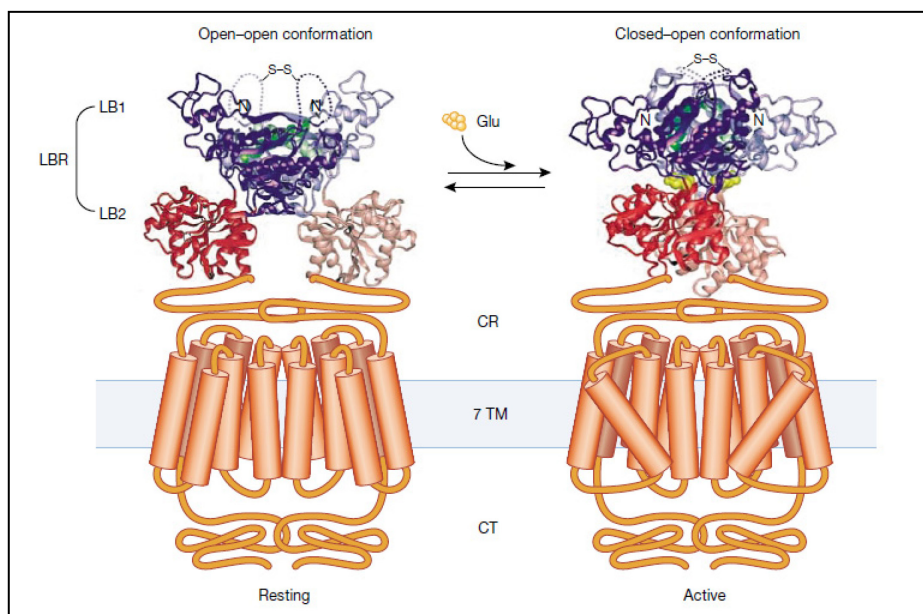


Figure 1.1: Structure of the mGluR1 homodimer

The mGluR homomer consists of a large extracellular N-terminal domain, seven transmembrane domains and a large intracellular C-terminal domain. Functional mGluRs are assembled into dimers. Without glutamate mGluRs adopt an open-open conformation, which represents the resting state. Binding of glutamate stabilizes the closed-open conformation and activates the receptor (taken from (Moepps and Fagni, 2003)).

Functional mGluR receptors are homodimers (Fig. 1.1), with each monomer consisting of a large N-terminal ligand binding domain (LBD), seven transmembrane domains (7TMD) and an intracellular C-terminal domain interacting with the trimeric G-protein and in multiple ways with proteins of the postsynaptic density (PSD) (Tu et al., 1999; Tu et al., 1998). Importantly, mGluRs together with other postsynaptic proteins including Homer form a multi-protein signaling complex (Nakamura et al., 2004). The cloning of the first metabotropic glutamate receptor, mGluR1a, led to the identification of this new family of G protein coupled receptors (GPCR) (Houamed et al., 1991; Masu et al., 1991). To date, seven other genes encoding mGluRs have been identified and the receptors are classified into three groups according to their amino acid sequence homology, downstream signal transduction pathways and pharmacological properties (Nakanishi, 1992) (Fig. 1.2). Group II and III mGluRs inhibit the adenylyl cyclase. Group I mGluRs constituted by mGluR1 and mGluR5 couple positively to phospholipase C (PLC) and their activation leads to generation of inositol - 3 - phosphate (InsP₃) and diacylglycerol (DAG).

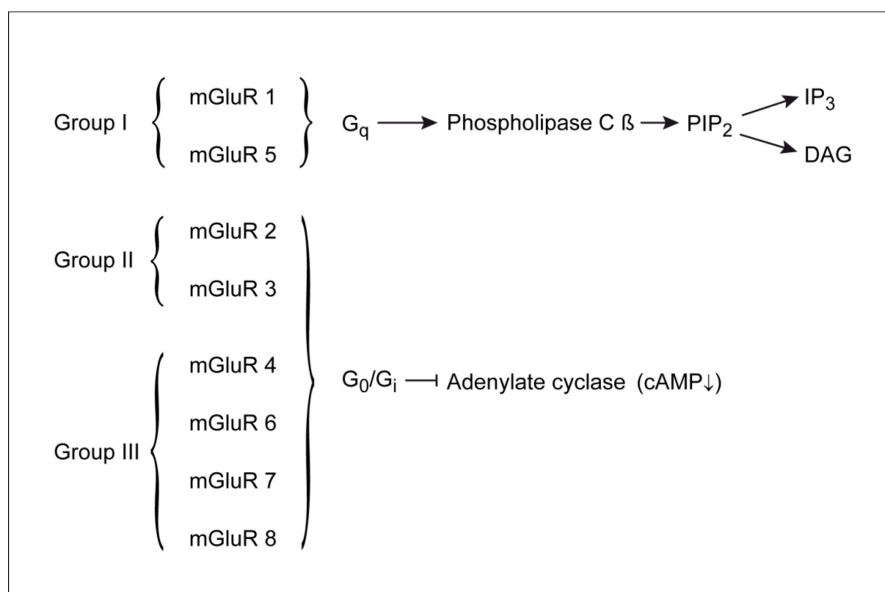


Figure 1.2: Classification of metabotropic glutamate receptors

mGluRs are classified into three groups, based on amino acid sequence homology, downstream signal transduction pathways and pharmacological properties (Nakanishi, 1992).

The metabotropic glutamate receptor 1 is expressed throughout the brain, with high expression levels in olfactory bulb, thalamus, hippocampus and cerebellum (Lein et al., 2007). However, of all different mGluR subtypes, the expression of mGluR1 is exceptionally high in cerebellar Purkinje cells (Fig.1.3) (Lein et al., 2007; Shigemoto et al., 1992).

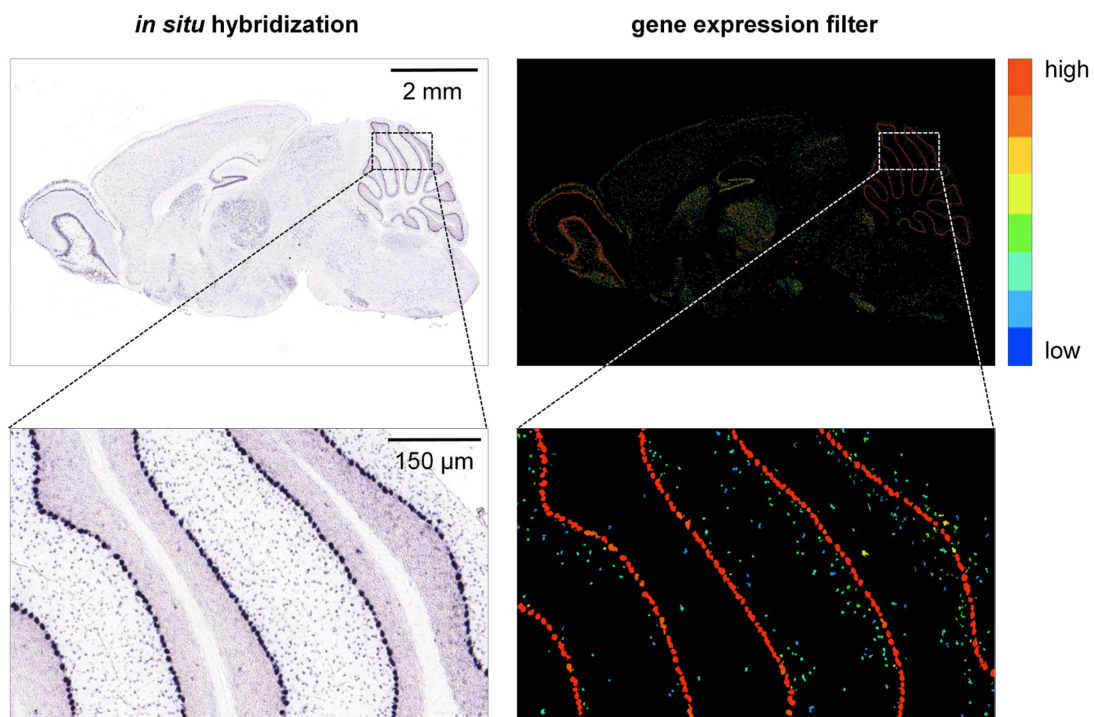


Figure 1.3: Expression of mGluR1 mRNA in the mouse brain

(Top) In-situ-hybridization of mGluR1 RNA in a whole brain preparation of the mouse (left) and after application of a gene expression filter (right).

(Bottom) Magnification of a cerebellar section reveals exceptionally high mGluR1 expression in Purkinje cells. (taken from: Allen Brain Atlas (<http://mouse.brain-map.org>)) Color scale in arbitrary units.

1.2 Purkinje cells

The most prominent neuronal element in the stereotyped cerebellar circuitry is the Purkinje cell (PC), first described by the Czech anatomist Jan Evangelista Purkyně in 1837. Purkinje cell somata are located in the Purkinje cell layer (PCL) separating the molecular layer (ML) from the granular layer (GL) (Fig. 1.4). The characteristic highly branched, planar dendritic tree emanating from the Purkinje cell somata extend in a sagittal plane into the molecular layer, where they establish synapses with 100.000 – 200.000 parallel fibers (PF) in which each parallel fiber forms only a weak excitatory input and with usually one climbing fiber (CF), which forms with 100 – 150 synaptic contacts at the proximal part of the Purkinje cell dendrite a strong excitatory input (Ito, 2006).

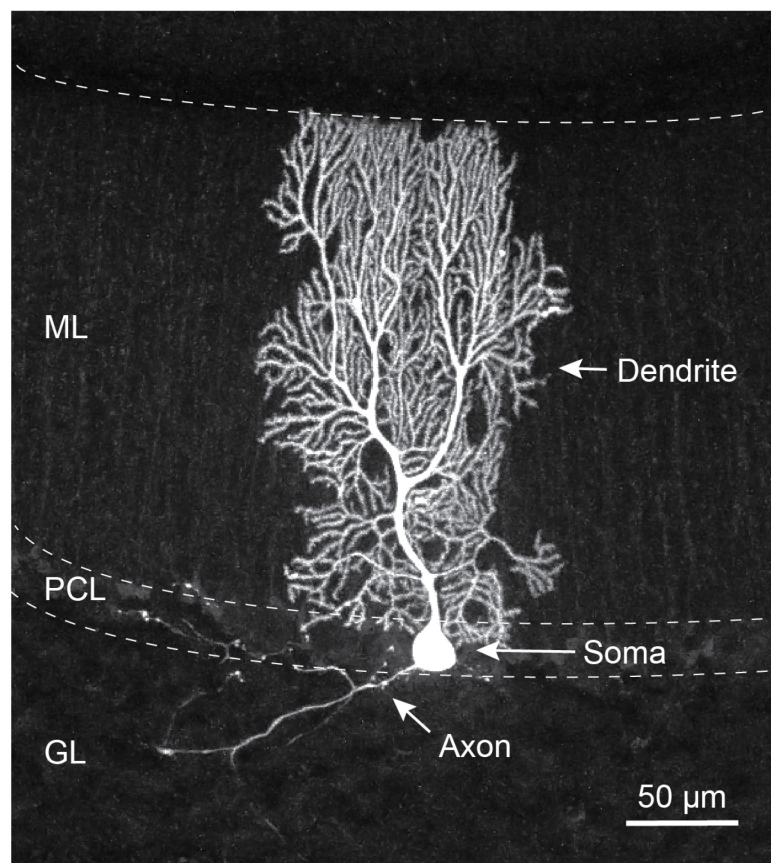


Figure 1.4: Cerebellar Purkinje cell in a slice preparation

Confocal image of a biocytin filled Purkinje cell in a slice of the mouse cerebellar vermis. Biocytin is labeled with streptavidin conjugated with Alexa 488. Purkinje cell somata are located in the Purkinje cell layer (PCL) emanating their planar, highly branched dendritic tree into the molecular layer. Below the PCL, granular cells are densely packed in the granular layer (GL), sending their axons into the molecular layer (ML) and form synaptic contacts with Purkinje cell spines. The axons of Purkinje cells project to cells in the deep cerebellar nuclei.

The axons of the Purkinje cells represent the sole output of the cerebellar cortex to the primary target, the deep cerebellar nuclei (DCN), where they form inhibitory GABAergic synapses with DCN neurons. The firing pattern of Purkinje cells represents the result of the entire signal processing and integration of the cerebellar cortex and is thus of outstanding importance for the function of the cerebellum.

1.3 mGluR1 and cerebellar function

The functions classically assigned to the cerebellum are motor coordination, fine tuning of movements and motor learning (Eccles, 1967; Ito, 2000, 2006). Interference with cerebellar function causes ataxia, which is characterized by incoordination of balance, gait and eye movements (Bastian, 1997; Duenas et al., 2006; Schmahmann, 2004). Functional expression of mGluR1 is indispensable for cerebellar function and hence for motor control. A comorbidity in human patients with Hodgkin lymphoma is paraneoplastic cerebellar ataxia, which has been shown to be associated with autoantibodies generated against mGluR1 (Sillevis Smitt et al., 2000). Compared to healthy humans these patients show a strong intention tremor during saccadic eye movements, one of the main symptoms of ataxia (Coesmans et al., 2003). Deletion of mGluR1 in a transgenic mouse model leads to a severe atactic phenotype (Aiba et al., 1994; Kano et al., 1997). By utilization of other genetic manipulations it could be shown, that mGluR1 expression in Purkinje cells is responsible for the motor deficits. Thus, the phenotype in the total mGluR1 knockout mouse can be rescued with selective mGluR1 expression in Purkinje cells in otherwise mGluR1-deficient mice (Ichise et al., 2000). Conversely, blockade of mGluR1 expression in adult mGluR1 conditional knockout mice, expressing mGluR1 selectively in Purkinje cells, leads again to an atactic phenotype (Nakao et al., 2007). In conclusion, these experiments show unambiguously the crucial role of mGluR1 expression in Purkinje cells for motor control.

The cerebellum is not only responsible for motor coordination, but also for learning and adjustment of motion sequences. Learning relies on plasticity of the underlying neuronal structures and besides morphological changes also physiological changes of synapses occur during this process. For parallel fiber to Purkinje cell synapses a direct connection between certain learning processes and a long lasting decline in AMPA receptor mediated transmission, denominated as long

term depression (LTD), has been demonstrated (Ito, 2001, 2002; Mauk et al., 1998). Induction of LTD requires repeated simultaneous activity of parallel fibers and the climbing fiber (CF) and the function of mGluR1 is crucial in the induction process. Deletion of mGluR1 in mice (Aiba et al., 1994) and application of mGluR1 blocker in vivo (Gao et al., 2003) prevents LTD induction.

The findings that the activity at the cerebellar output depends on mGluR1 expressed at Purkinje cell synapses leads to the question how mGluR1 is involved in synaptic transmission at these synapses.

1.4 Synaptic transmission at parallel fiber synapses

The glutamatergic transmission at the parallel fiber to Purkinje cell synapse is quite unique in the central nervous system because functional NMDA receptors are not expressed there (Shin and Linden, 2005). A contribution of NMDA receptors to the climbing fiber response has been demonstrated recently (Piochon et al., 2007; Renzi et al., 2007). However, no NMDA receptor activation can be detected after parallel fiber activation. The synaptic transmission at the parallel fiber-Purkinje cell synapse relies on AMPA and mGluR1 receptors (Konnerth et al., 1990; Llano et al., 1991; Takechi et al., 1998). The two glutamate receptors types are located differently at postsynaptic sites. Whereas the AMPA receptors are to be found at the center of the synapse, opposite of the release site (Masugi-Tokita et al., 2007; Nusser et al., 1994), mGluR1 receptors are concentrated perisynaptically (Baude et al., 1993; Nusser et al., 1994), at the periphery of the synapse. The difference in subcellular localization of the two receptor types is also reflected in the mode of activation. AMPA receptors are easily activated by glutamate released after excitation of parallel fibers with a single shock stimulus (Konnerth et al., 1990; Llano et al., 1991). The AMPA receptor-mediated depolarization leads to activation of voltage gated Ca^{2+} channels (VGCC) if a sufficient number of parallel fibers is activated (Eilers et al., 1995). The opening of VGCCs, mostly of the P/Q type, is followed by an elevation of intracellular Ca^{2+} concentration (Eilers et al., 1995).

Repetitive parallel fiber stimulation is necessary to attain sufficiently high levels of glutamate in the synaptic cleft for the activation of mGluR1 at the periphery of the synapse (Batchelor and Garthwaite, 1993, 1997; Batchelor et al., 1994; Takechi et al., 1998; Tempia et al., 1998). Granule cells generate prolonged bursts of action potentials (APs), with firing frequencies of up to 1kHz, following sensory stimulation (Chadderton et al., 2004; Jörntell and Ekerot, 2006). Thus, the

transmission between granule cells and Purkinje cells is well suited for mGluR1 activation under physiological conditions. In *in vitro* experiments it has also been demonstrated, that parallel fiber presynaptic boutons are able to follow this frequency (Brenowitz and Regehr, 2007).

Binding of glutamate to mGluR1 launches two independent pathways leading to release of Ca^{2+} ions from intracellular stores and to slow influx of cations from the extracellular space (Fig. 1.5). The signaling cascade linking mGluR1 to Ca^{2+} release involves activation of PhospholipaseC β (PLC β) which cleaves phosphoinositol 4,5-bisphosphate (PIP₂), thus generating inositol 1,4,5-trisphosphate (InsP₃) and diacylglycerol (DAG). Binding of InsP₃ to Ca^{2+} permeable InsP₃ receptors (InsP₃R) in the membrane of the endoplasmic reticulum (ER) finally leads to Ca^{2+} release from the ER into the cytosol (Finch and Augustine, 1998; Takechi et al., 1998).

The first evidence for a second mGluR1-dependent signal came from experiments demonstrating a slow depolarizing potential (sEPSP or sEPSC) following activation of mGluR1 (Batchelor and Garthwaite, 1993; Batchelor et al., 1994). The mechanism responsible for the generation of the sEPSP was unknown. It was shown that both signals, the Ca^{2+} transient and the sEPSC, require $\text{G}\alpha_q$ (Hartmann et al., 2004). Despite intensive research, the identity of the channel mediating the sEPSP has long remained unresolved. It had been demonstrated that the sEPSC is carried by Na^+ ions (Knöpfel et al., 2000) and Ca^{2+} ions (Canepari et al., 2004) and that the underlying channel has a low open probability and a single channel conductance of 0.6 pS (Canepari et al., 2004). The mGluR1-dependent inward current reverses at ~ 20 mV, which is characteristic for an unspecific cation conductance, (Canepari et al., 2001; Kim et al., 2003). All these properties point to a member of the canonical transient receptor potential (TRPC) channel and a previous publication suggested TRPC1 as the mediator of the sEPSC (Kim et al., 2003). This result was challenged by the finding that the sEPSC persists in combined absence of TRPC1 and TRPC4, indicating that none of these subunits is required for sEPSC mediation (Hartmann et al., 2008).

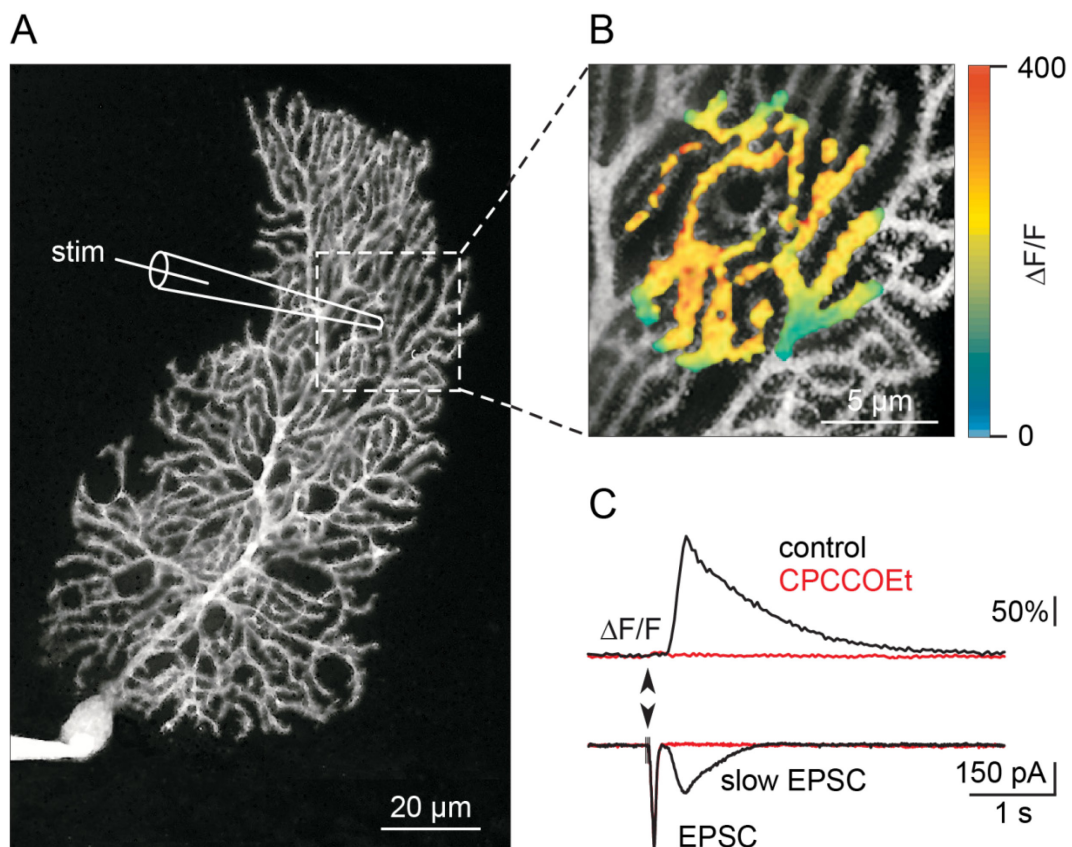


Figure 1.5: mGluR1 mediated signaling at the parallel fiber-Purkinje cell synapse

(A) Confocal image of a whole cell patch clamped Purkinje cell in an acute sagittal slice of the cerebellar vermis. The Purkinje cell was filled with the Ca^{2+} indicator OGB-1 via the patch pipette. Parallel fibers were electrically stimulated with a stimulation pipette (stim) placed on top of the slice in some distance from the Purkinje cell dendrites. **(B)** The site of electrical stimulation at higher magnification. The increase of intracellular Ca^{2+} concentration after repetitive parallel fiber stimulation is highlighted with false colors. **(C)** Black traces: Repetitive parallel fiber stimulation (5 stimuli at 200Hz with $10\mu\text{M}$ CNQX present in the bath) evokes an increase in intracellular Ca^{2+} concentration (top) and two excitatory postsynaptic currents, a fast one and a slow one (bottom). Red traces: The Ca^{2+} transient and the slow EPSC are abolished after application of the specific mGluR1 blocker CPCCOEt ($200\mu\text{M}$).

1.5 Transient Receptor Potential Channels in Purkinje cells

The first *transient potential channel* (TRP) was discovered in a *Drosophila* mutant displaying a transient receptor potential to continuous light exposure (Minke, 1977; Montell et al., 1985). Since then many other TRP channels have been described, founding a new channel superfamily. The TRPs are divided into two groups and further separated into seven subfamilies based on amino acid sequence homology and topological differences. Group 1 contains TRPC, TRPV, TRPM, TRPN and TRPA and group 2 members are TRPP and TRPML (Venkatachalam and Montell, 2007). All TRP channels have in common that they serve functions in sensory physiology in sensing of sound, light, chemicals, temperature and touch (Clapham, 2003).

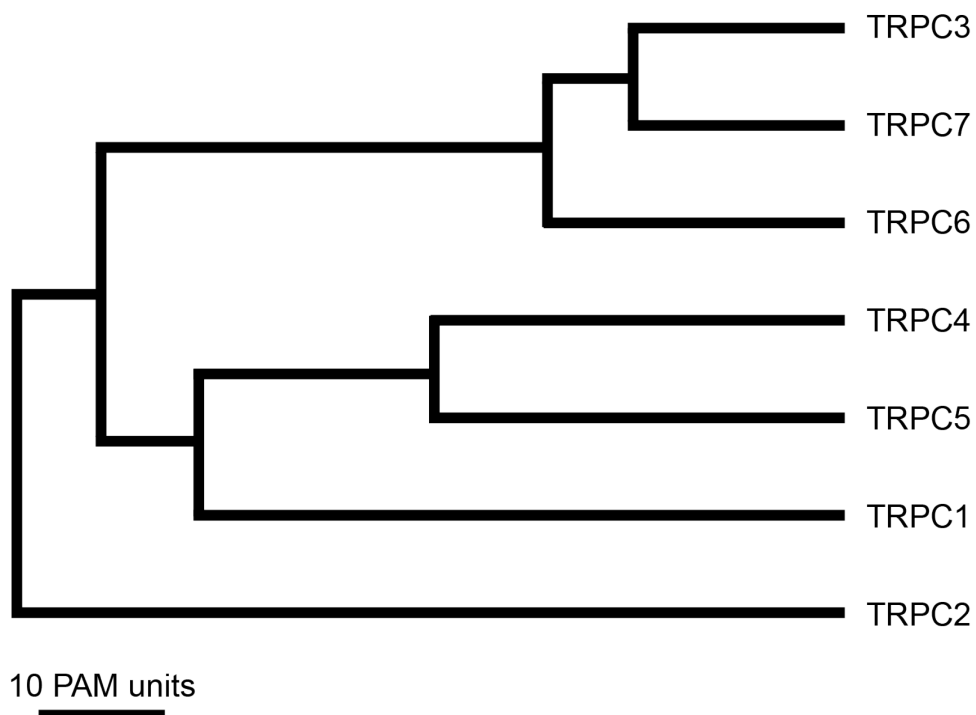


Figure 1.6: Phylogenetic tree of the TRPC subfamily

The evolutionary distance is shown by the total branch lengths in point accepted mutations (PAM) units, which is the mean number of substitutions per 100 residues (adapted from (Clapham et al., 2001)).

The TRPC subfamily has the closest relation to *Drosophila* TRP channel (Ramsey et al., 2006) and the first mammalian TRP homologues identified were TRPC1, TRPC2 and TRPC3 (Wes et al., 1995; Zhu et al., 1995). Currently, four additional TRPC proteins have been described, referred to as TRPC4-TRPC7 (Montell et al., 2002). Based on sequence similarities the TRPCs are divided into four subgroups, with TRPC1, TRPC2, TRPC3/6/7 and TRPC4/5 as components of each group (Fig. 1.6) (Venkatachalam and Montell, 2007). The molecular architecture of each TRPC protein consists of six transmembrane domains (TMD), with the putative pore forming region situated between the fifth and sixth transmembrane segment. The TMD are flanked by intracellular C - and N - terminal domains (Vannier et al., 1998). The common feature of TRPC channels is the formation of tetramers activated downstream of G protein coupled receptors and the PLC (Putney, 2004; Villereal, 2006). They have been implicated in many processes, including sensory processing (Tai et al., 2009; Talavera et al., 2008). However, the functions of TRPC channels in the CNS were unclear. With the exception of TRPC2 (Huang et al., 2007; Liman et al., 1999; Zufall, 2005), all TRPC subunits are expressed in the brain (Lein et al., 2007). In the cerebellum likewise all subunits are expressed. The expression profile of TRPCs in the cerebellum of rats between P0 and P42 shows a constant expression of TRPC1 in contrast to a significant up-regulation of TRPC3 and significant down-regulation of TRPC4 and TRPC6 (Huang et al., 2007). With the use of quantitative real-time RT-PCR it was demonstrated that in the cerebellum, TRPC1 and TRPC3 are equally abundant (Dragicevic, 2008). In contrast to single Purkinje cells where TRPC3 is the by far dominating TRPC subunit, with an eight to ten fold higher mRNA expression in comparison to TRPC1 (Dragicevic, 2008). TRPC3 proteins are mainly found in Purkinje cell somata and dendrites (Hartmann et al., 2008; Huang et al., 2007).

1.6 Aim of the study

The aim of this study was to characterize mGluR1-dependent synaptic signaling at cerebellar parallel fiber to Purkinje cell synapses by using whole-cell patch-clamp recordings combined with confocal or two-photon Ca^{2+} imaging. In particular, mGluR1-mediated currents should be tested in mice lacking distinct TRPC channel subtypes in order to verify suggestions about a possible involvement of TRPC channels in slow synaptic transmission in Purkinje cells. The contribution of the mGluR1-dependent unspecific cation conductance to postsynaptic Ca^{2+} signaling was to be analyzed. For this purpose, a novel AOD-based two-photon scanning system was to be implemented and utilized for the first time for a detailed analysis of Purkinje cell spine mGluR1-dependent Ca^{2+} signaling. Finally, different hypotheses regarding the function of the sEPSC for Purkinje cell processing of synaptic activity were to be tested.

2 Materials and Methods

A combination of whole-cell patch clamp recordings and fluorescence microscopy was used for measurements of Ca^{2+} transients in dendrites and single spines of cerebellar Purkinje cells in acute cerebellar slices. The methods of brain slice preparation, patch clamp recordings, Ca^{2+} imaging and the corresponding materials are described in detail in this chapter.

2.1 Animals

All experiments were carried out in accordance with institutional animal welfare guidelines of the government of Bavaria, Germany. Mice with a deletion of Exon7 in the TRPC3 gene (Hartmann et al., 2008) as well as TRPC1-deficient mice (Dietrich et al., 2007) were bred in the animal facility of the Institute of Neuroscience. C57/BL6 wild type mice were used as controls. The mice were reared in a 12 hours light/dark cycle and kept with food and water *ad libitum*. The age of the animals used for experiments ranged from P25 to P180.

2.2 Solutions and Pharmacology

For slice preparation and perfusion of slices during experiments artificial cerebrospinal fluid (ACSF) containing (in mM) 125 NaCl, 4.5 KCl, 2 CaCl_2 , 1 MgCl_2 , 1.25 NaH_2PO_4 , 26 NaHCO_3 , and 20 glucose with an osmolarity of ~ 315 mosm was used. The ACSF was prepared at the beginning of an experimental day.

The internal solution (IS) for patch clamping was prepared on a weekly basis as a stock solution and stored at -20°C . Before usage the IS stock was melted and diluted (80:20 IS/ H_2O) to the final concentration. The calcium indicator Oregon Green BAPTA - 1 (Molecular Probes, USA) was added in the 20% portion to the IS. Finally, the ready-for-use IS was filtered with a $0.2\mu\text{m}$ filter device (Millipore, USA). The composition of the final IS was as follows in mM: 148 K - gluconate, 10 HEPES, 10 NaCl, 0.5 MgCl_2 , 4 Mg-ATP, 0.4 $\text{Na}_3\text{-GTP}$, and 0.1 Oregon Green BAPTA-1 (Molecular Probes, USA). The pH was adjusted to 7.3 with 3M KOH and the osmolarity was tested to be ~ 310 mosm. For some experiments also 0.2% Biocytin (Sigma, Germany) was included in the IS.

For the experiments following pharmacological agents were used according to requirements. To block GABA_A receptor-mediated transmission, 10 mM bicuculline

(Axxora; Germany) was included as default to the circulating ACSF. To isolate mGluR1 receptor mediated signaling, the fast glutamatergic transmission via AMPA receptors was inhibited, if not otherwise stated, with 40 μ M 6-Cyano-7-nitroquinoxaline-2,3-dione disodium (CNQX) (Ascent Scientific; UK). For depletion of intracellular stores the SERCA blocker 30 μ M cyclopiazonic acid (CPA) (Sigma; Germany) was used. Direct activation of mGluR1 was achieved by local pressure ejection (10psi; 100ms) of 200 μ M of the group 1 agonist 3,5-Dihydroxyphenylglycine (DHPG) (Tocris; USA). In experiments in which DHPG was applied also 100nM tetrodotoxin (TTX) (Ascent Scientific; UK) was present in the bath. In order to block mGluR1 receptors, 200 μ M of the noncompetitive mGluR1 specific antagonist 7-(Hydroxyimino)cyclopropa(b)chromen-1a-carboxylate ethylester (CPCCOEt) (Sigma; Germany) was used.

2.3 Brain slice preparation

Acute slices from the cerebellar vermis were prepared in accordance with the animal care and use guidelines of the government of Bavaria, Germany.

Acute cerebellar slices were prepared according to standard procedures (Edwards et al., 1989; Llano et al., 1991). The mice were anesthetized with CO₂ and decapitated. Starting from caudal at the level of the cervical medulla to rostral ending at bregma ~ -1mm bilateral incisions and a frontal incision of the cranium were performed. The epicranium was removed and the cerebellum and part of the cerebrum were laid open. After two paramedian sagittal cuts at the level of the cerebellar hemispheres, one horizontal cut at the base of skull (basis crania interna) and a horizontal cut through the cerebrum (bregma ~ -1mm) the cerebellar vermis was rapidly dissected and placed in ice-cold ACSF (0°C – 2°C) bubbled with 95% O₂ and 5% CO₂. Using cyanoacrylate based superglue (UHU Sekundenkleber, Bühl/Germany) one lateral side of the tissue block was glued to a stage, placed into a slicing chamber and subsequently submerged in ice-cold oxygenated ACSF. Parasagittal slices of the cerebellar vermis with a thickness of 300 to 350 μ m were cut using a vibratome slicer (Leica VT1200S, Wetzlar/Germany). In order to increase the quality of the slices the built-in Vibrocheck function of the slicer was used in order to minimize vertical vibrations of the blade (Geiger et al., 2002). The cut slices were transferred to an oxygenated storage chamber and kept for 30 to 45 minutes at 34°C (Edwards et al., 1989). Finally the slices were stored in ACSF at room temperature for up to 8 hours.

For experimental recordings one slice was transferred to a recording chamber and mechanically fixed at the bottom of the recording chamber with a grid of nylon threads glued to a U-shaped platinum frame. During the entire experiment the slice was continuously perfused (perfusion rate 2 – 2.5 ml/min) with ACSF containing 10 μ M bicucullin in order to block GABA_A receptors. All experiments were performed at room temperature.

Purkinje cells near the surface of the slice were identified based on their location in the Purkinje cell layer and their morphology (size and shape of the somata).

2.4 Electrophysiology

Whole-cell recordings were performed following standard procedures (Edwards et al., 1989). Recordings were obtained with an EPC8 or EPC10 amplifier (HEKA; Germany) and the 'Pulse' software (HEKA; Germany) was used for data acquisition. Patch pipettes (3–4M Ω) were pulled on a DMZ universal puller (Zeitz-Instrumente; Germany) from borosilicate glass (Hilgenberg; Germany). For experiments with the EPC8 amplifier the patch pipettes were additionally coated with silicon (RTV 615; GE Silicons). During the recordings, the slices were continuously perfused at room temperature with ACSF. Afferent stimulation was performed using a patch pipette filled with 1 M NaCl (1 M Ω resistance). The stimulation pipette was placed in the molecular layer, 15 – 50 μ m above or below the Purkinje cell target dendrite. Stimuli were applied by a triggered isolated pulse stimulator (Model 2100; A-M Systems; USA) with pulses (150 μ s duration) of 1.5 to 25V. The liquid junction potential for the used IS and ACSF was calculated to be 14.5 mV and was left uncorrected. Following gigaseal formation the pipette capacitance was canceled and the whole-cell configuration was attained with application of short negative pressure pulses to the pipette. The membrane capacitance was compensated after establishing the whole-cell configuration. The series resistance (R_s) which ranged from 5 to 12 M Ω was not compensated. Data were sampled at 20kHz and filtered with a 10kHz Bessel filter.

2.5 Fluorescence microscopy

For monitoring the intracellular calcium concentration two different imaging systems were used. In the following section these two systems are briefly explained.

2.5.1 Spinning disk confocal microscopy

A multi-point confocal microscope using dual spinning disc technology (QLC 100; VTi; UK), attached to an upright microscope (E600FN; Nikon; Japan) and equipped with 40x objective (NIR Apo, NA 0.8; Nikon; Japan) was used to acquire fluorescence images from dendritic fields in parallel to the patch clamp recordings.

This system allows recordings with a high sensitivity and temporal resolution at the cost of spatial resolution.

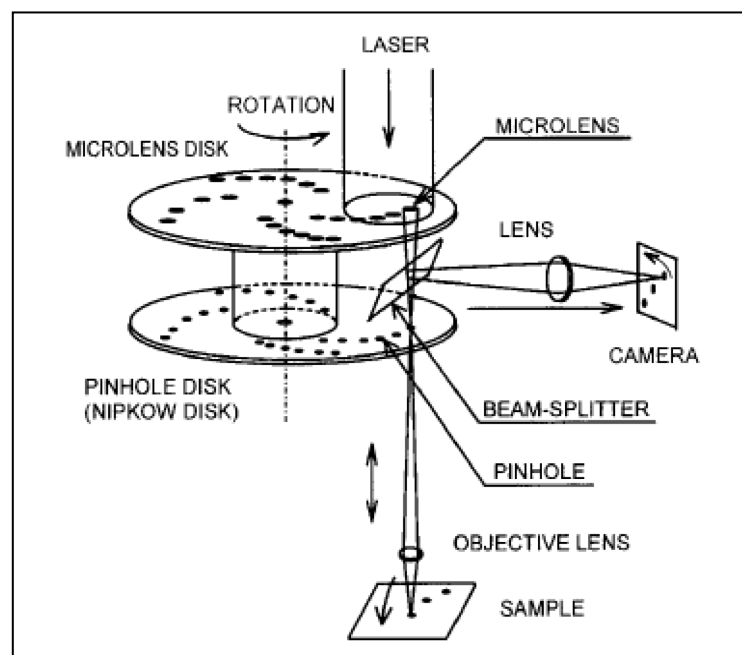


Figure 2.1: Schematic of a dual spinning disc multi-point scanner

An expanded and collimated laser beam is projected onto a dual spinning disc. The upper disc contains an array of microlenses focusing the excitation light onto the corresponding pinhole at the lower disc. After passing the pinhole the excitation light is focused with an objective onto the sample. The emitted light is projected back onto the pinhole and reflected to a detector via a dichroic mirror. The microlenses and corresponding pinholes are arranged in a spiral pattern in that fashion, that each 30° the field of view is fully scanned with the parallel beams. At a fixed speed of the discs of 30 rotations per second, 360 frames per second can be acquired. (taken from (Inoue and Inoue, 2002))

One-photon excitation was generated by a Sapphire laser (Coherent; USA) with a wavelength of 488nm and adjustable output power of up to 75 mW. Full-frame 80x80 pixel images were recorded at 40 Hz with a CCD camera (NeuroCCD, RedShirt imaging, USA). Synchronization of the spinning disc with the CCD camera was achieved by utilization of a function generator (TG1010A; TTI; UK). For data acquisition, the commercially available software Neuroplex (RedShirt imaging, USA) was used.

2.5.2 AOD - based two photon microscopy

Calcium signals in dendritic spines were imaged with a custom-built two photon laser scanning microscope (for more details, see (Leischner, 2011)). This newly developed scanning system is ideal for monitoring fluorescent signals in compartments as small as dendritic spines. A standard upright microscope (BX50WI, Olympus) was equipped with the scanning device and a 63x objective (Plan Apochromat; NA 1; Zeiss; Germany). A pulsed Titanium-Sapphire laser was used for two-photon excitation (Chameleon Ultra; Coherent; USA) set to 800 nm and tuned to 140 fs, with a pulse repetition rate of 80MHz. The laser beam was steered in x direction by a fast acousto-optical deflector (4150; Crystal Technology; USA) and in y direction by a slower galvanic mirror (6215H, Cambridge Technology; USA). The group velocity dispersion (also called 'chirp'), caused by the glass of the optics and the TeO₂ crystals of the AOD, was corrected with a pulse compressor (FemptoControl; APE; Germany). The chromatic dispersion of the scanning AOD (AOD2) was compensated by a second AOD (AOD1, model 4150; Crystal Technology; USA) (Salome et al., 2006). An additional custom compensation optics was inserted behind the scanning AOD to compensate for beam distortions caused by the non-homogeneous grating due to fast scanning (for details see (Leischner, 2011)) A suited dichroic mirror (HC 735 LP; AHF Analysentechnik AG; Germany) was mounted into the filter cube to separate the emission light from the two-photon excitation light, reflecting wavelength between 350-720nm towards the PMT, and allowing for an unrestricted transmission of wavelengths between 750-1100nm. The scanning mirror, the AOD and the data acquisition with the digitizer ran in synchronicity, controlled by a custom-written software (Leischner, 2011) based on LabVIEW (LabVIEW 2009, National Instruments; USA). The pixel clock was running at 20MHz, resulting in a 50ns pixel dwell time. The microscope can run with an

image frequency between 20 and 1000 Hz, and field of views between 10 and 100 μm . These different imaging configurations are controlled by different sets of parameters, optimized for different frame rates and field of views. A configuration with 320 images per second (250 x 250 Pixel) with a field of view of 15 μm x 15 μm was mainly selected in experiments performed in this study. At the end of each experiment, a z-stack of the examined dendritic segment was recorded (15 μm x 15 μm , 320 Hz; step size in depth-direction: 250 nm). During the acquisition, the data was continuously written to the hard disc in a suited streaming format. To conduct the offline analysis, the data were reloaded, downsampled to a predefined image frequency, and automatically saved as an image sequence.

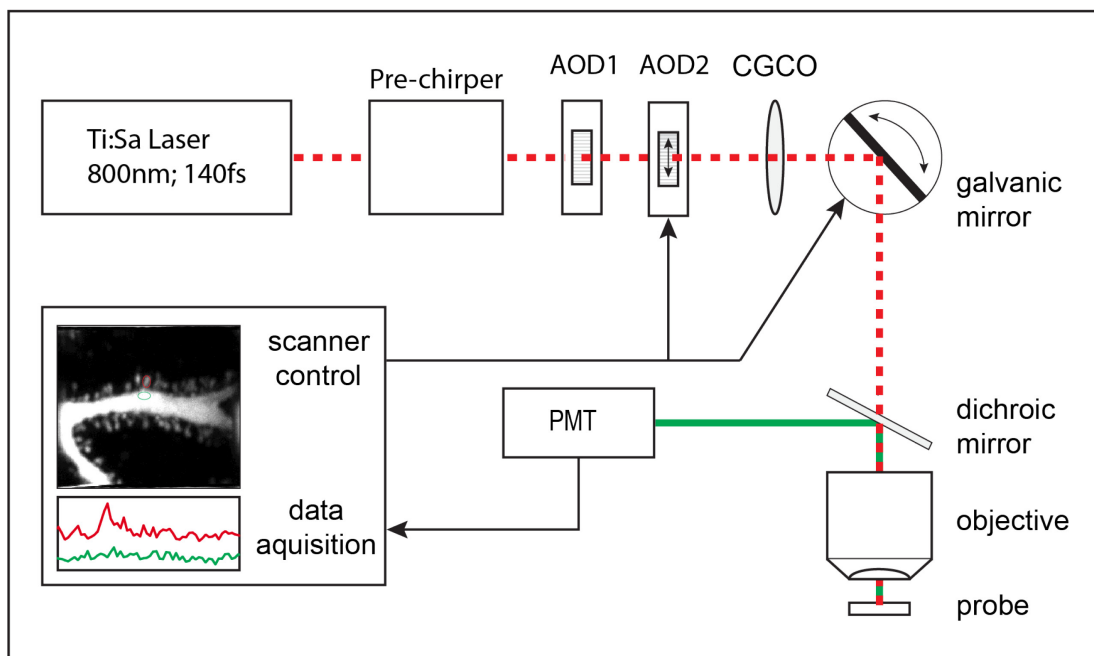


Figure 2.2: Schematic diagram of the AOD based two photon scanning system

Two-photon excitation is generated by a pulsed Titan:Sapphire laser. In order to scan a sample, the laser beam is steered in x-direction by an acousto-optical deflector (AOD2) and in y-direction by a galvanic mirror. Chromatic and temporal distortions of the beam are compensated by utilization of a beam compressor (pre-chirper), a second AOD (AOD1) and the chirped grating compensation optics (CGCO). The excitation light is focused to a fluorescent sample by an objective. The emitted light is captured by the same objective lens, separated from the excitation pathway by a dichroic mirror and detected with a photomultiplier tube (PMT).

2.5.3 Ca²⁺ indicator

To measure the dynamic change in the intracellular calcium concentration the cell-impermeant fluorescent Ca²⁺ indicator Oregon Green 488 BAPTA-1 (OGB1) was used. With a dissociation constant (K_d) of 380nM at 24°C (Yasuda et al., 2004), OGB1 belongs to the high affinity dyes and is therefore well suited to report small changes in Ca²⁺ concentration. The maximum for one-photon excitation lies at 494 nm and for two-photon excitation the dye is best excited at 800-810 nm (Haugland et al., 2005). Additionally, OGB1 absorbs two-photon excitation more efficiently as comparable dyes, which reduces the necessary laser intensity and therefore reduces photodamage (Paredes et al., 2008). Independent of the mode of excitation the peak of the emission spectrum is 523 nm.

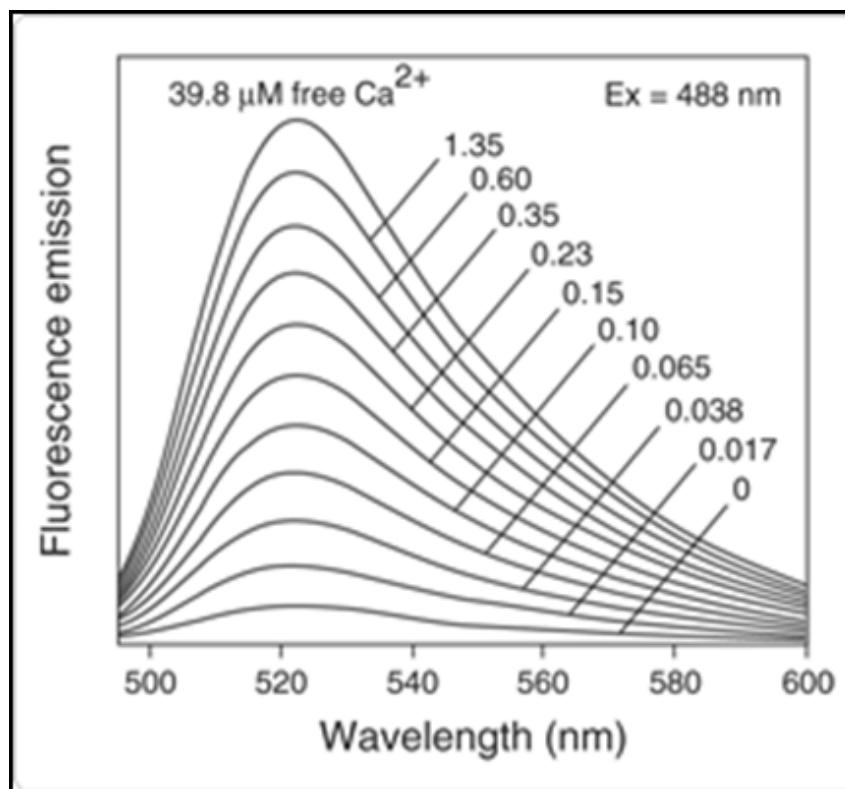


Figure 2.3: Fluorescence emission spectrum of Oregon Green 488 Bapta1

The fluorescence emission spectrum depends on the free Ca²⁺ concentration and the emitted wavelength. The dye is best excited at 494 nm and the optimal emission wavelength can be found at 523nm. (taken from (Haugland et al., 2005))

Ca²⁺ changes of up to ~1,4μM have been reported following certain regimes of repetitive parallel fiber stimulation in spines of Purkinje cells (Wang et al., 2000). Because the dynamic range of OGB-1 is ~14 (Haugland et al., 2005) it has to be considered that dye saturation could occur when Ca²⁺ changes become maximal. The advantage of OGB-1 is that it displays a high fluorescence at resting Ca²⁺ concentration, even in response to low excitation intensity, which allows to identify even small structures as Purkinje cell dendritic spines without the risk of photodamage.

2.6 Analysis

For further analysis, the acquired image sequences were converted into a tagged image file format (TIFF). Conversion of data acquired with the spinning disc system was done with commercial software (Neuroplex; RedShirt; USA) and data from the AOD based two photon system was done with custom written LabVIEW software.

Determination of the region of interest (ROI) and readout of raw data traces was done with ImageJ (<http://www.macbiophotonics.ca/imagej/index.htm>). Igor Pro (Wavemetrics, USA) and the Igor Pro plugins, Patcher's Power tool (<http://www.mpibpc.mpg.de/groups/neher/index.php?page=software>) and Neuromatic (<http://www.neuromatic.thinkrandom.com>) were used for final analysis. Throughout this study the fluorescence (F) is normalized to resting fluorescence (F₀) and expressed as relative fluorescence change over time ($\Delta F/F = (F - F_0)/F_0$).

The kinetic parameters shown in 3.8 and 3.11 were determined as follows (see also Fig. 2.4). The decay time constant was measured by a monoexponential fit from the peak to the end of the trace. Rise time was determined from 10% to 90% of the peak and the delay was measured from the beginning of the stimulation to the point of the rising phase which was closest to one standard deviation of the baseline. The amplitude was determined after smoothing the traces with a binomial algorithm with factor 1.

All values are reported as means ± SEM. Statistical significance was tested using paired or unpaired Student's t test. The criterion for significance was p < 0.01.

The figures and pictures were constructed and arranged using Adobe Illustrator and Adobe Photoshop (Adobe Systems, USA).

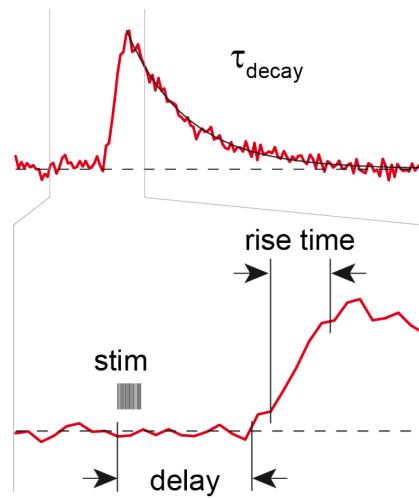


Figure 2.4: Determination of kinetic parameters of Ca²⁺ transients

Averaged trace of Ca²⁺ signals evoked with sparse parallel fiber stimulation (SPFS), recorded during one experiment. The decay time constant, delay, rise time and amplitude was measured as indicated.

3 Results

3.1 mGluR1 – mediated signaling is intact in the absence of TRPC1

To verify claims about a role of TRPC1 in synaptic transmission at parallel fiber synapses (Kim et al., 2003) mGluR1-dependent signaling was tested in TRPC1-deficient mice (Dietrich et al., 2007). To avoid interference with possible presynaptic changes in the general knockout, short pressure pulses of the group I mGluR-specific agonist DHPG (200 μ M for 100ms at 10psi) were locally applied to dendritic regions of Purkinje cells.

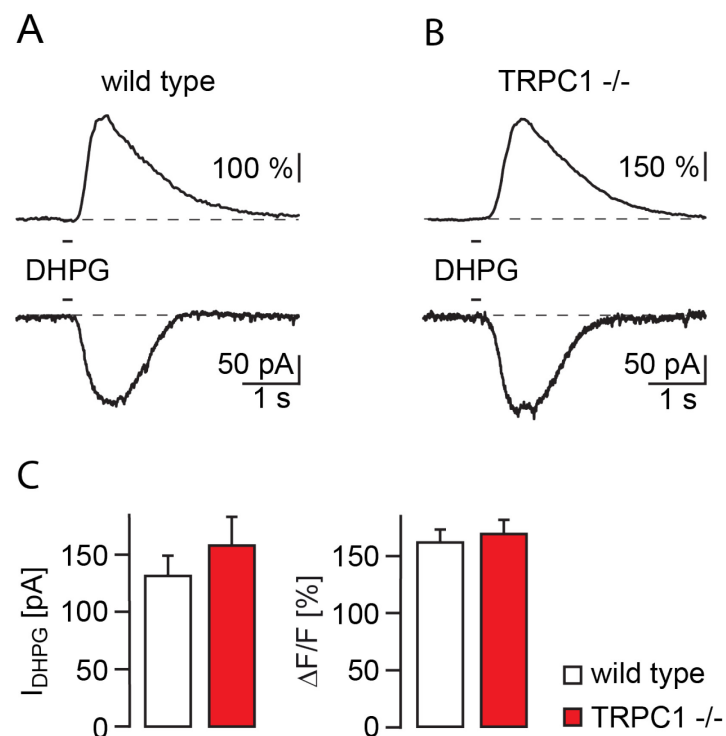


Figure 3.1: mGluR1 mediated signaling in absence of TRPC1

(A) mGluR1 dependent Ca²⁺ transient (top) and inward current (bottom) following local application of the group I mGluR-specific agonist DHPG via pressure ejection (200 μ M for 100ms at 10psi) in wild type mice. **(B)** Similar experiment performed in TRPC1 -/- mice. **(C)** Summary of the DHPG-evoked current (left) and Ca²⁺ transient (mean \pm SEM; wild type n = 38 dendritic regions from 15 cells in 5 animals and TRPC1-/- n = 30 dendritic regions from 14 cells in 4 animals).

In both wild type and TRPC1 $-/-$ mice, a Ca^{2+} transient and inward current were evoked by DHPG-ejection (Fig. 3.1A and 3.1B) with no discernible differences in the analyzed amplitudes (Fig. 3.1C). Thus, in contrast to earlier suggestions (Kim et al., 2003) TRPC1 is not the mediator of the sEPSC in cerebellar Purkinje cells of adult mice.

3.2 The mGluR1 dependent current is abolished in the absence of TRPC3

The most abundant TRPC subunit in Purkinje cells is TRPC3. On average, its expression outweighs that of TRPC1 by a factor of ten (Dragicevic, 2008). The working hypothesis that TRPC3 mediates the mGluR1-dependent sEPSC was tested in TRPC3-deficient mice.

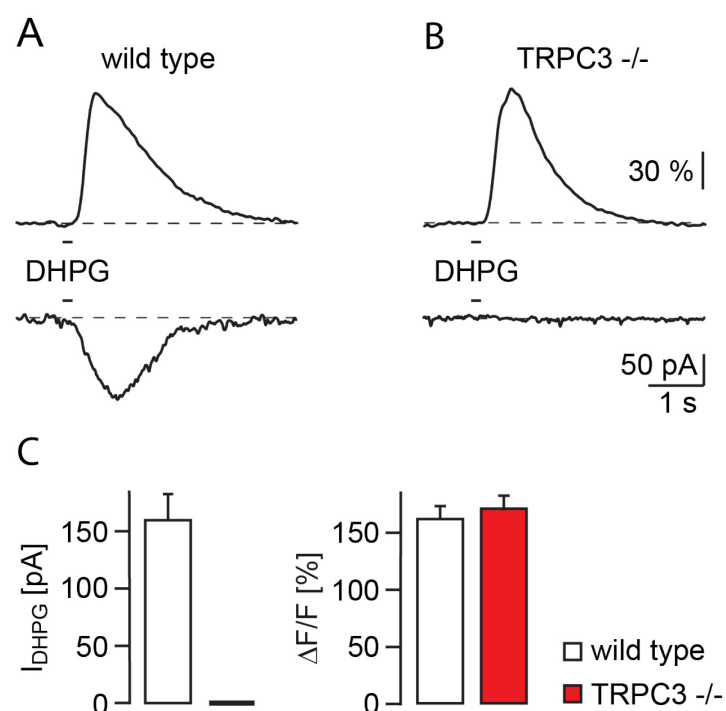


Figure 3.2: mGluR1 mediated signaling in absence of TRPC3

(A) mGluR1-dependent Ca^{2+} transient (top) and inward current (bottom) evoked by local application of DHPG via pressure ejection ($200\mu\text{M}$ for 100ms at 10psi) in wild type mice. **(B)** Similar experiment performed in TRPC3 $-/-$ mice revealed the absence of the inward current. **(C)** Summary of the DHPG-evoked current (left) and Ca^{2+} transient (mean \pm SEM; wild type $n = 26$ dendritic regions from 10 cells in 2 animals and TRPC3 $-/-$ $n = 30$ dendritic regions from 14 cells in 4 animals).

Local pressure ejection of DHPG (200 μ M for 100ms) to Purkinje cell dendrites in TRPC3-deficient mice revealed no difference in the mGluR1-mediated Ca²⁺ signal, compared to the signal in wild type mice (Fig. 3.2A, 3.2B top and 3.2C right) The mGluR1-dependent inward current, in contrast, was completely absent in all TRPC3 -/- mice tested (Fig. 3.2A, 3.2B bottom and 3.2C left).

3.3 The Ca²⁺ transient in the absence of TRPC3 is mediated by mGluR1-dependent Ca²⁺ release from internal Ca²⁺ stores

In order to confirm that the Ca²⁺ signal recorded in TRPC3 -/- mice (Fig. 3.3A left and 3.3C left) is indeed a mGluR1 mediated Ca²⁺ release from internal stores, mGluR1 was activated using the more physiological repetitive parallel fiber stimulation (10 stimuli at 100Hz). To avoid contamination of the mGluR1-mediated Ca²⁺ signal with Ca²⁺ influx through voltage-gated Ca²⁺ channels (Eilers et al., 1995; Hartmann et al., 2004; Takechi et al., 1998), the fast synaptic transmission mediated by AMPA receptors was completely abolished using a high CNQX concentration (40 μ M). Under these conditions, application of the mGluR1 antagonist CPCCOEt (200 μ M) totally blocked the recorded Ca²⁺ transient (Fig. 3.3A and 3.3B).

The same result was achieved by depleting internal stores using the sarcoplasmic/endoplasmic reticulum Ca²⁺ ATPase (SERCA) antagonist CPA (30 μ M) (Garaschuk et al., 1997; Kovalchuk et al., 2000). The Ca²⁺ transient stimulated in control condition (Fig. 3.3C left) was abolished in the presence of CPA (Fig. 3.3C right and Fig. 3.3D).

The absence of the response after these two pharmacological interventions clearly indicates that the measured Ca²⁺ transient in Purkinje cell dendrites of TRPC3 -/- mice represents Ca²⁺ release from internal stores downstream of mGluR1 activation.

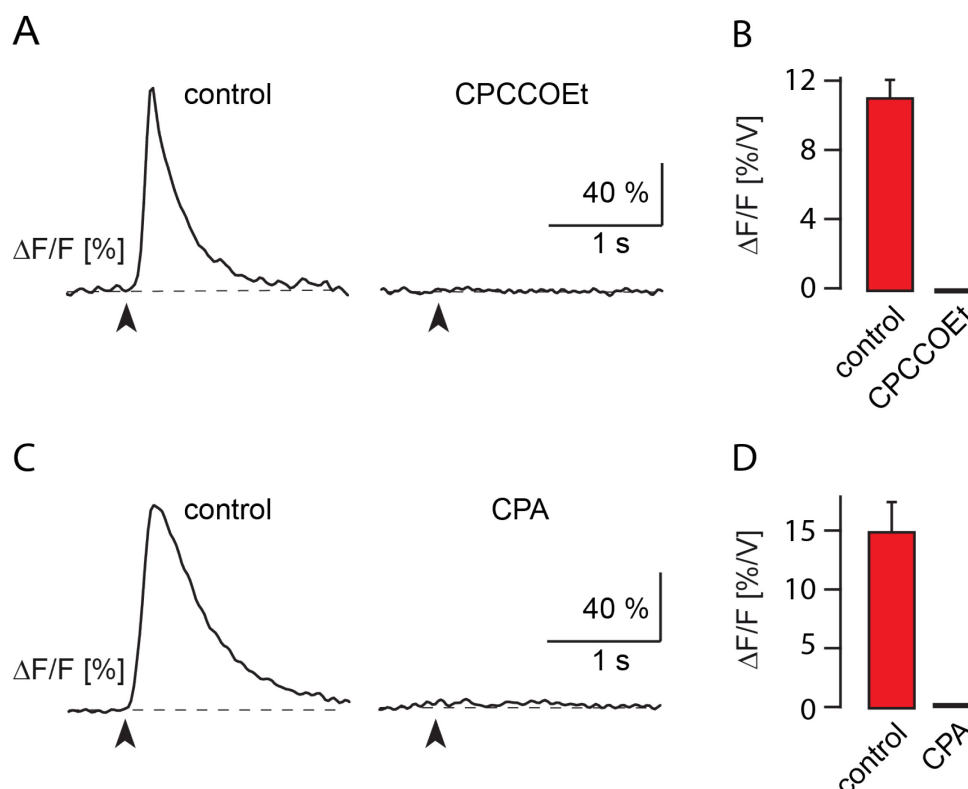


Figure 3.3: mGluR1 mediated Ca²⁺ release in TRPC3 deficient mice

(A) Repetitive synaptic parallel fiber stimulation (10 stimuli at 100Hz) in TRPC3 ^{-/-} mice evoked a Ca²⁺ transient (left) which was blocked by application of the mGluR1 specific blocker CPCCOEt (200μM; right). **(B)** Summary of the response in control condition and in the presence of CPCCOEt, normalized to the strength of stimulation (n = 4 cells). **(C)** mGluR1 dependent Ca²⁺ signal evoked by repetitive parallel fiber stimulation (10 stimuli at 100Hz) is abolished by application of the blocker of SERCA pumps CPA (30μM). **(D)** Summary of the response in control conditions and after application of CPA, normalized to the strength of stimulation (n = 6 cells).

3.4 AMPA receptor-mediated EPSCs are normal in the absence of TRPC3

To test for possible changes in fast synaptic transmission mediated by AMPA receptors at the parallel fiber-Purkinje cell synapse in TRPC3 ^{-/-} mice, characteristic features of AMPA receptor-mediated EPSCs (Konnerth et al., 1990) were determined. Purkinje cells were whole-cell voltage-clamped and AMPA receptor-dependent EPSCs evoked by single-shock stimulation of parallel fibers (Eilers et al., 1995; Takechi et al., 1998).

As in wild type mice, fast synaptic transmission in TRPC3 $-/-$ mice is completely blocked in the presence of the antagonist of AMPA receptors CNQX (40 μ M) (Fig. 3.4A and 3.4B). Single shock-evoked EPSCs had similar monoexponential decay time constants in TRPC3 $-/-$ (12.9 ± 0.9 ms, $n = 11$ cells) and in wild type mice (11.6 ± 0.7 ms, $n = 8$ cells; $p = 0.31$) indicating that the time course of AMPA receptor-dependent signaling is not altered by the deletion of TRPC3.

Increasing the stimulus strength of parallel fiber stimulation results in a gradual increase of postsynaptic responses due to increasing the number of activated parallel fibers (Konnerth et al., 1990). For the elucidation of the stimulus intensity-response relation the strength of the electrical stimulation was increased from 0V to 10V in 1V steps and the amplitude of the AMPA receptor-mediated EPSC was measured in wild type mice (Fig. 3.4C top) and TRPC3 $-/-$ mice (Fig. 3.4C bottom). The plot of EPSC amplitudes against stimulus strength reveals no significant difference between the two genotypes (Fig. 3.4D).

Parallel fiber-Purkinje cell synapses are characterized by paired-pulse facilitation (PPF) (Konnerth et al., 1990). PPF of parallel fiber to Purkinje cell synapses was tested in TRPC3-deficient mice and compared to PPF observed in cerebellar slices of wild type mice. For that, Purkinje cells were whole-cell patch-clamped and parallel fibers were stimulated twice at interstimulus intervals (ISIs) of 0.05, 0.1, 0.2, 0.5 and 1s. By dividing the amplitude of the second EPSC by the amplitude of the first EPSC the paired-pulse ratio (PPR) was obtained. In wild type mice, the PPR at an ISI of 50ms was 180% and declined with increasing ISI length to 102% at 500ms. Similarly, in TRPC3 $-/-$ mice PPR at an ISI of 50ms was 183% and declined to 102% at an ISI of 500ms. No significant difference of the PPR at the different ISI was found. Thus, compared to the wild type, PPF is not altered in TRPC3 $-/-$ mice (Fig. 3.4E and 3.4F) indicating that presynaptic glutamate release is very likely not affected by the deletion of TRPC3.

All in all, these data provide evidence for normal AMPA receptor-dependent synaptic transmission in the absence of TRPC3.

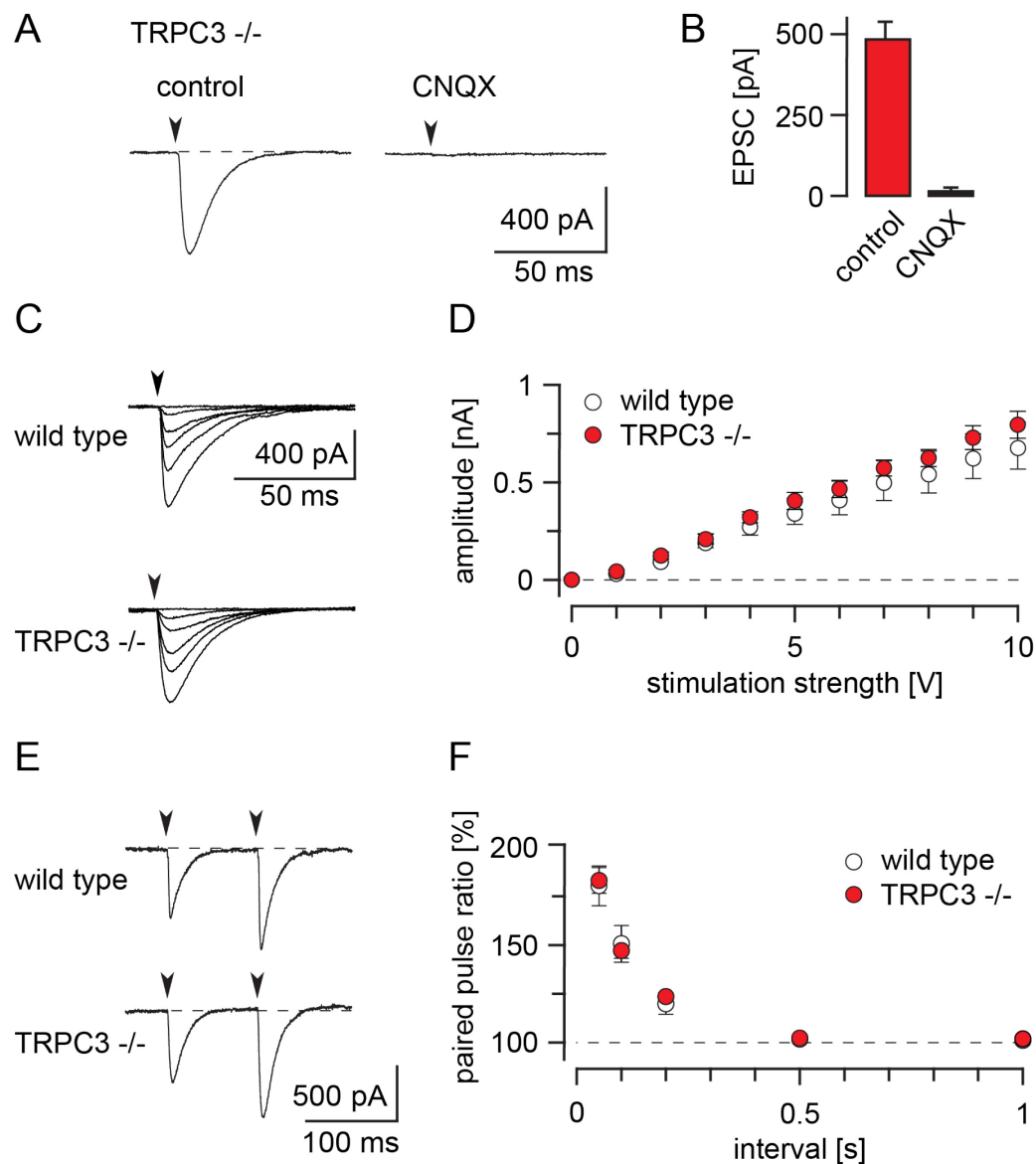


Figure 3.4: Characterization of AMPA receptor-mediated fast synaptic transmission in TRPC3-deficient mice

(A) Fast AMPA receptor-mediated EPSC evoked by a single shock synaptic stimulation in TRPC3 $-/-$ mice (left) is blocked by application of the AMPA receptor antagonist CNQX (40 μ M; right). **(B)** Summary of the response in control condition and in the presence of CNQX ($n = 5$ cells) **(C)** AMPA receptor-mediated responses to single shock stimulation of increasing strength (0 – 10V in 2V steps) in wild type mice (top) and TRPC3 $-/-$ mice (bottom). **(D)** Summary of the graded response in wild type mice (white dots, $n = 9$ cells) and TRPC3 $-/-$ mice (red dots, $n = 11$ cells). **(E)** Fast EPSCs in response to paired parallel fiber stimulation (100ms interval) in wild type mice (top) and TRPC3 $-/-$ mice (bottom). **(F)** Summary of the time course of paired pulse facilitation in wild type mice (white dots, $n = 8$ cells) and TRPC3 $-/-$ mice (red dots, $n = 11$ cells).

3.5 Two synaptic Ca^{2+} signaling components downstream of mGluR1

TRPC3 is a Ca^{2+} -permeable unspecific cation channel (Groschner and Rosker, 2005). To reveal a possible TRPC3-dependent intracellular Ca^{2+} elevation in response to synaptic mGluR1 activation, the internal store, was depleted with the use of cyclopiazonic acid (CPA, 30 μM).

Similarly to earlier experiments, Purkinje cells in cerebellar slices were whole-cell patch-clamped and filled with 100 μM OGB-1. Repetitive parallel fiber stimulation in the presence of 40 μM CNQX was followed by a sEPSC (Fig. 3.5A bottom) and a transient local increase in intracellular Ca^{2+} concentration (Fig. 3.5A top) recorded with confocal imaging. This Ca^{2+} transient is characterized by a steep rise of Ca^{2+} and large amplitude (10 stimuli @ 100Hz: 124 \pm 18%; 20 stimuli @ 200Hz: 169 \pm 12 n=7 cells) in control conditions (Fig. 3.5A top). After 20 minutes of exposure to 30 mM CPA in the bath, mGluR1-dependent Ca^{2+} release is abolished due to depletion of ER Ca^{2+} stores (see Fig. 3.13). Under these conditions, when the same stimulation parameters are used, a slow and small CPA-resistant Ca^{2+} signal (10 stimuli @ 100Hz: 21 \pm 2%; 20 stimuli @ 200Hz: 31 \pm 4 n=7 cells) is revealed. The amplitude of this “residual” Ca^{2+} transient is about ~ 20% of the amplitude of Ca^{2+} transients recorded in control conditions (Fig. 3.5B top and 3.5C). The amplitude and time course of the sEPSC, in contrast, is not affected by CPA (compare Fig. 3.5A bottom with 3.5B bottom and 3.5D). It has been shown before that the amplitude of the sEPSC depends on the number of pulses applied and on the frequency of the burst, with response saturation at 200Hz in slices (Tempia et al., 1998). To maximally activate the mGluR1 dependent pathway leading to activation of TRPC3, repetitive stimulation with 20 stimuli at 200Hz were applied. This “maximal” stimulation increased the compound Ca^{2+} signal (control condition), the sEPSC (control condition and CPA) and the CPA resistant Ca^{2+} component significantly (Fig. 3.5C and 3.5D).

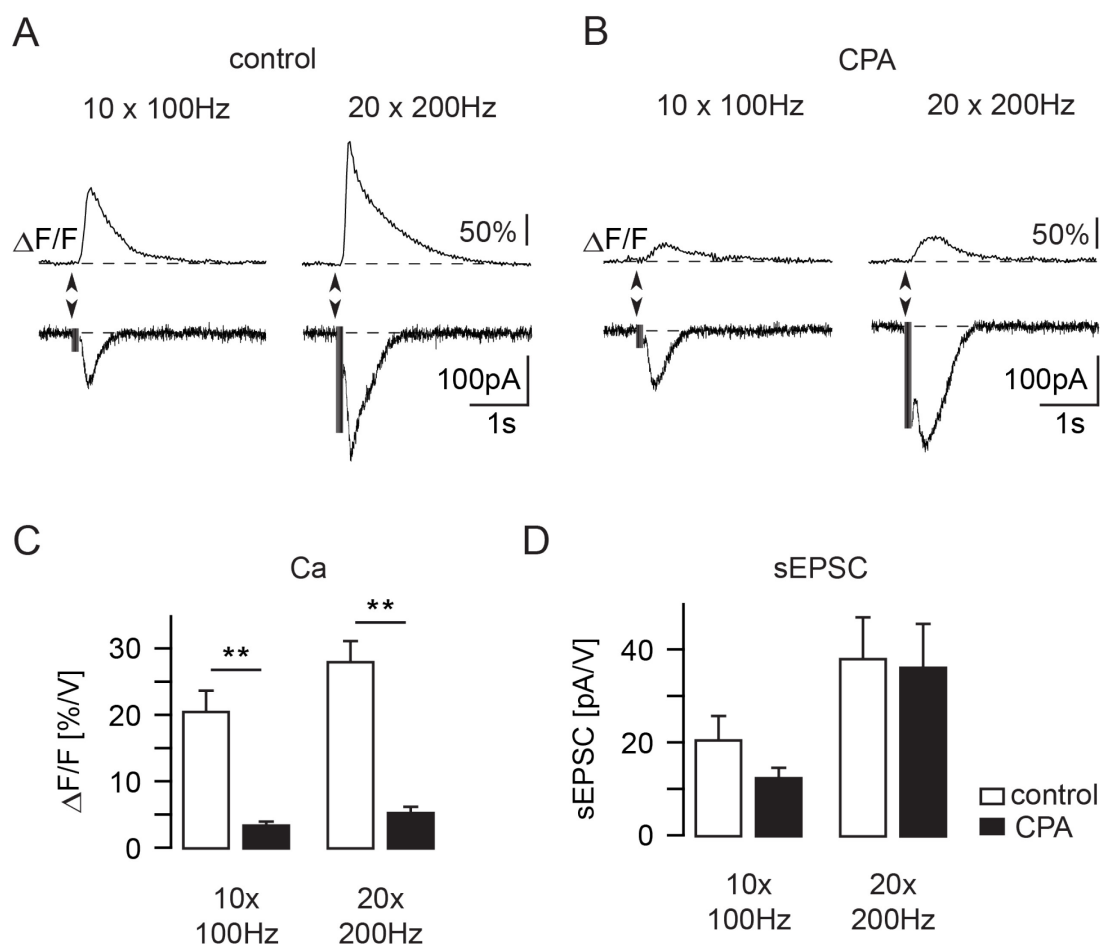


Figure 3.5: Depletion of internal stores reveals a residual Ca^{2+} component

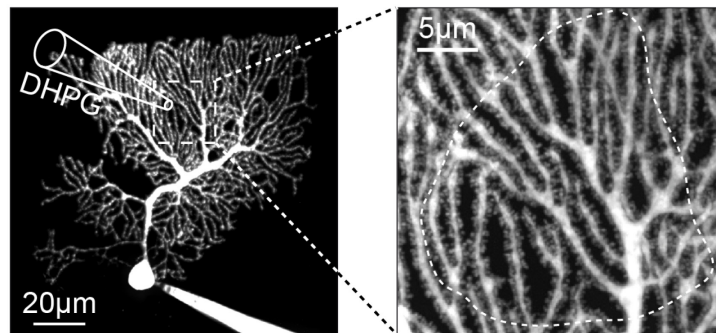
(A) Ca^{2+} - transients (top) and sEPSC (bottom) evoked by repetitive parallel fiber stimulation with 10 stimuli at 100 Hz (left) and 20 stimuli at 200 Hz (right) in control condition. **(B)** Depletion of internal Ca^{2+} stores with CPA (30 μM) reveals a CPA-resistant Ca^{2+} component (top) without affecting the sEPSC (bottom). **(C)** Summary of Ca^{2+} responses ($n = 7$ cells) normalized to stimulation strength in control conditions (white bargraphs) and in the presence of CPA (black bargraphs) with two stimulation regimes. **(D)** Summary of sEPSC ($n = 7$ cells) normalized to stimulation strength in control conditions (white bar graphs) and in the presence of CPA (black bar graphs) with two stimulation regimes (** - highly stat. dif., $p=0.001$).

3.6 Two components of agonist-evoked mGluR1-dependent dendritic Ca²⁺ signals

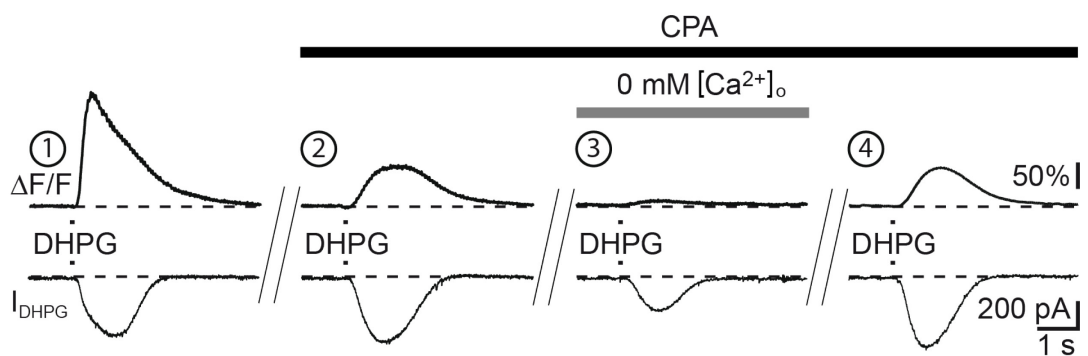
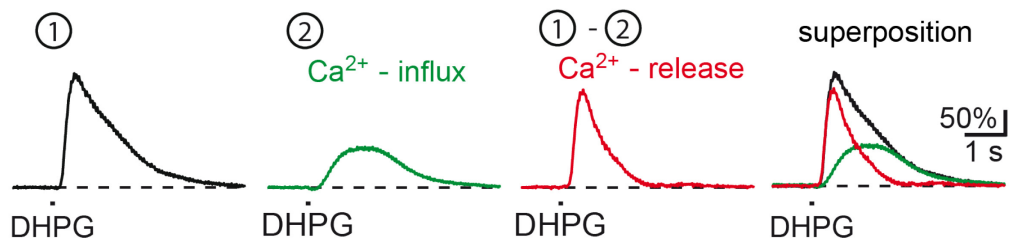
In order to test in Ca²⁺-free ACSF whether the CPA-resistant Ca²⁺ signal depends on extracellular Ca²⁺ DHPG (200µM with 10psi in 100ms) was used for the activation of mGluR1-dependent responses. As already demonstrated in section 3.1 and 3.2, DHPG was locally pressure-ejected to dendrites of Purkinje cells (Fig. 3.6A) and under control conditions this evoked an mGluR1-dependent Ca²⁺ transient recorded with confocal fluorescence imaging (Fig. 3.6B① top). Concomitantly, an inward current was recorded with somatic whole-cell patch-clamp (Fig. 3.6B① bottom). The following depletion of internal stores with CPA (30 µM for at least 20 min) had no effect on the mGluR1-dependent inward current (Fig. 3.6B② bottom) and did not abolish the DHPG-evoked Ca²⁺ signal. However, the Ca²⁺ transient was reduced to a great extent (Fig. 3.6B② top). The time course of the residual smaller Ca²⁺ signal closely follows the time course of the inward current (Fig. 3.6B②). Removal of Ca²⁺ from the ACSF abrogates the calcium transient almost completely, sparing ~53% of the inward current (Fig. 3.6B③ and 3.6D right). Both signals recover after readdition of Ca²⁺ ions to the external solution (Fig. 3.6B④ and 3.6E), indicating that the CPA-resistant Ca²⁺ signal is a Ca²⁺ influx from the extracellular space. As demonstrated in Fig. 3.6C the control Ca²⁺ signal and the CPA-resistant Ca²⁺ transient were used to calculate the shape of the pure Ca²⁺ release signal from internal stores. Subtraction of the Ca²⁺ influx signal ② from the compound Ca²⁺ signal ① results in a Ca²⁺ transient with slightly reduced amplitude and faster decay (Fig. 3.6C), demonstrating that the CPA-resistant Ca²⁺ influx influences the kinetics of the overall mGluR1 mediated Ca²⁺ signal.

To show unambiguously that the CPA-resistant Ca²⁺ influx is tightly associated with TRPC3 function at the parallel fiber-to-Purkinje cell synapse the analogous experiment as in Fig. 3.6 was performed in TRPC3-deficient mice. The mGluR1-dependent Ca²⁺ transient could be evoked by local pressure ejection of DHPG without the associated inward current (Fig. 3.7B left traces). After depletion of internal stores with CPA (30µM) the mGluR1 dependent Ca²⁺ signal was completely abolished (Fig. 3.7B right traces), demonstrating that the Ca²⁺ transient, recorded in control conditions in TRPC3-deficient mice, is a pure release signal from intracellular stores and, furthermore, the CPA-resistant Ca²⁺ influx component recorded in wild type mice is a TRPC3-mediated Ca²⁺ influx.

A



B Consecutive DHPG-applications

C MGluR1-dependent Ca^{2+} signaling components

D

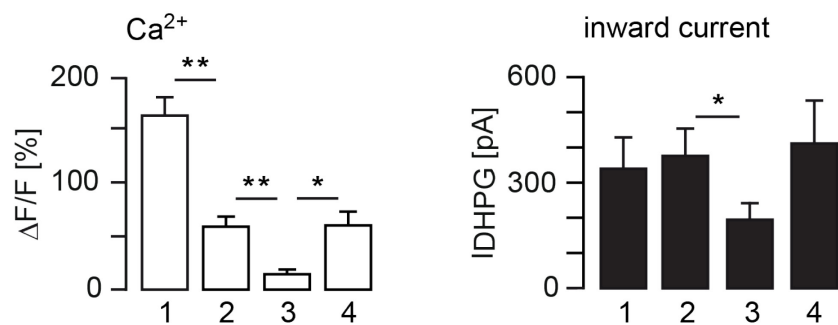


Figure 3.6: CPA-resistant Ca^{2+} response represents a Ca^{2+} influx signal

(A) Left: Confocal image of a patch-clamped Purkinje cell in a cerebellar slice from a wild type mouse. Right: The site of DHPG application at higher magnification. The dashed line encloses the dendritic region activated by short pressure ejection of DHPG (200 μM for 100 ms). (B) ① Pressure-ejection of DHPG evoked a slow inward current (I_{DHPG} ; lower trace) and a local Ca^{2+} -transient (upper trace). ② In the presence of 30 μM CPA in the bath, I_{DHPG} persisted, while the dendritic Ca^{2+} -transient was strongly reduced. ③ Reduction of I_{DHPG} and abolition of the dendritic Ca^{2+} transient in nominal Ca^{2+} -free external solution in the presence of CPA. ④ Recovery of both signals after readdition of Ca^{2+} ions to the external solution. (C) Dissection of the two components of mGluR1-dependent Ca^{2+} -signaling. Black – DHPG-evoked dendritic Ca^{2+} -signal shown in (B①), green – CPA-resistant Ca^{2+} -influx-transient shown in (B②), red – Ca^{2+} -release component: the result of the subtraction of the green from the black transient. (D) Summary of DHPG-evoked inward current and Ca^{2+} measurements. Bargraphs show mean signal amplitudes, (* - stat. diff., $p < 0.01$; ** - highly stat. diff., $p = 0.001$).

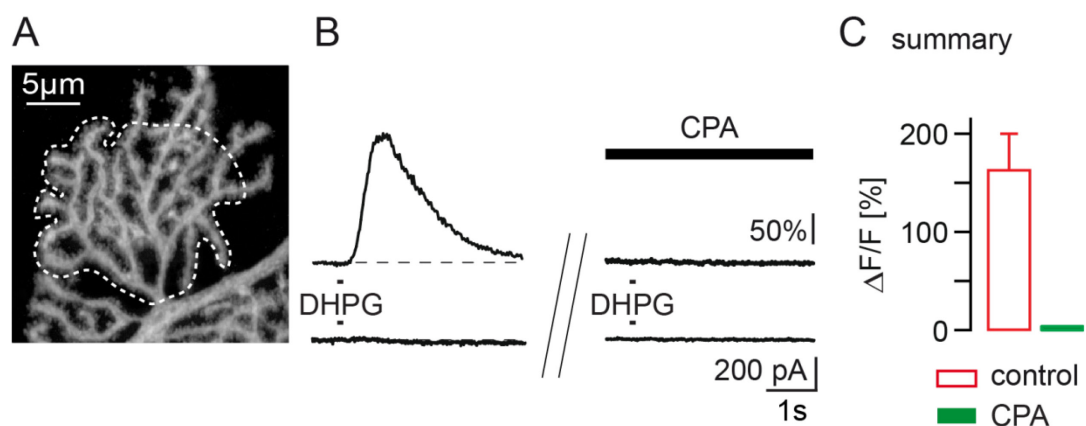


Figure 3.7: CPA resistant Ca^{2+} component is absent in TRPC3-deficient mice

(A) Confocal image of a part of a dendritic tree of a patch-clamped Purkinje cell filled with Oregon Green BAPTA-1 from a TRPC3-deficient mouse. The dashed line indicates the region activated by local pressure ejection of DHPG (200 μM , 100 ms). (B) Upper traces: Ca^{2+} transient evoked in response to the DHPG-application under control conditions (left) and in the presence of 30 μM CPA (right). The lower traces show the simultaneously recorded voltage clamp measurement. (C) Summary of Ca^{2+} measurements in TRPC3 $^{-/-}$ mice. Bargraphs show mean signal amplitudes of relative fluorescence changes ($\Delta F/F$).

3.7 Synaptic mGluR1-dependent Ca^{2+} signals in Purkinje cell spines

If TRPC3 as a Ca^{2+} -permeable channel is synaptically activated downstream of mGluR1 it should have an impact on Purkinje cell spine Ca^{2+} signaling. In order to be able to record Ca^{2+} signals in spines, greater spatial resolution than provided by confocal imaging was required. For that, a novel two-photon imaging device that utilizes an acousto-optical deflector (AOD) for laser beam steering was used (see 2.5.2, (Leischner, 2011)).

After patching and filling of a Purkinje cell with Oregon green BAPTA-1 (100 μM), the dendritic tree was scanned manually for a target dendrite with discernible lateral spines (Fig. 3.8A). A stimulation pipette was placed on top or below in some distance ($> 15\mu\text{m}$) from the dendrite under investigation. The “maximal” stimulation, described in Fig 3.5 (20 stimuli at 200Hz), was applied with a stimulation amplitude adjusted according to the mode of stimulation. With sparse parallel fiber stimulation only a small number of synaptic inputs are stimulated in contrast to dense parallel fiber stimulation where a bundle of fibers were activated. At the end of each experiment the laser intensity was increased and a z-stack of the targeted dendritic area was taken. Post hoc, the z-stack of the imaged dendritic area was deconvoluted and 3D reconstructed (Fig. 3.8A bottom right). From the 3D reconstruction it becomes obvious that the dendritic compartment is all over occupied by spines, protruding up- and downwards, and remaining invisible in the original recorded plane of focus (Fig. 3.8A). This has consequences for signals measured in the dendritic compartment, leaving the subcellular localization of the signal undistinguishable and resulting in a compound spine/dendrite signal. Therefore, only Ca^{2+} signals from spines sticking out laterally and discriminable from each other, were analyzed.

For imaging responses to sparse parallel fiber stimulation (SPFS) inputs at the periphery of the dendritic tree of Purkinje cells were chosen. Following sparse parallel fiber stimulation, mGluR1-dependent Ca^{2+} transients in single, dispersed spines could be repeatedly evoked in a subset of spines (Fig. 3.9A) without a corresponding signal in the dendritic compartment (Fig 3.9C) and neighboring spines. This demonstrates that a single Purkinje cell spine provides all necessary components for the synaptic activation of the mGluR1dependent compound Ca^{2+} signal. In these measurements it can be assumed that only few synapses are

activated and hence a sEPSC recorded at the soma is not discernible (Fig. 3.9C bottom), probably due to filtering out of the sEPSC in the dendrite.

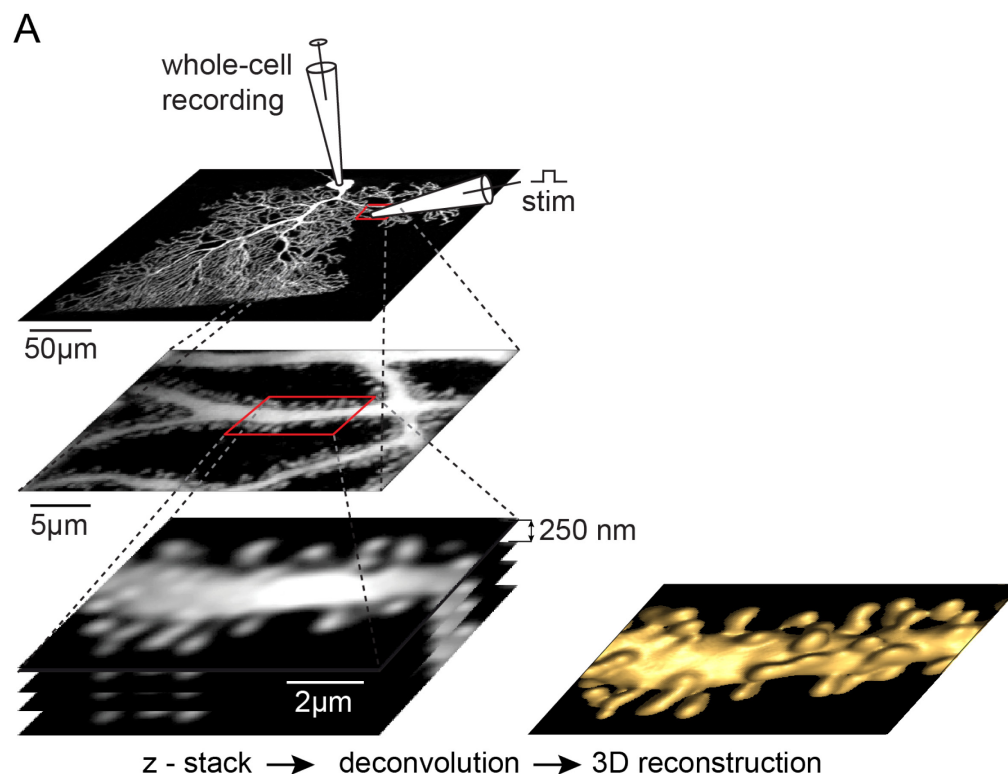


Figure 3.8: Two photon imaging of mGluR1 mediated Ca^{2+} signaling in Purkinje cell spines

(A) Confocal z-stack of a biocytin filled Purkinje cell (top left) zoomed in to the imaged spiny dendrite (middle left and bottom left). Purkinje cells were patched and filled with OGB1 via the patch pipette and stimulation pipette was placed in some distance on top or below the target dendrite. After recordings a z-stack was taken from the imaged area (bottom left, 250nm distance in z direction) and post hoc deconvoluted and reconstructed (bottom right).

In contrast to SPFS the Ca^{2+} -transients activated by DPFS are not restricted to single spines but span the entire dendritic branchlet. The Ca^{2+} transient recorded in the dendritic compartment (D_{all}) is as large as in the spines (Fig. 3.10C). Considering the large spine density demonstrated in the 3D reconstruction (Fig. 3.8 bottom right), the signal measured in the dendritic compartment can be considered as a composite signal containing spine and denditic components as mentioned

above. Furthermore, a Ca^{2+} transient could be reliably evoked during the course of the experiment in every spine analyzed. In this mode of stimulation with a higher number of synapses activated and probably also due to stronger activation of perisynaptically located mGluR1 due to glutamate spillover from neighboring synapses (Marcaggi and Attwell, 2005), a small sEPSC can be detected (Fig. 3.10C bottom).

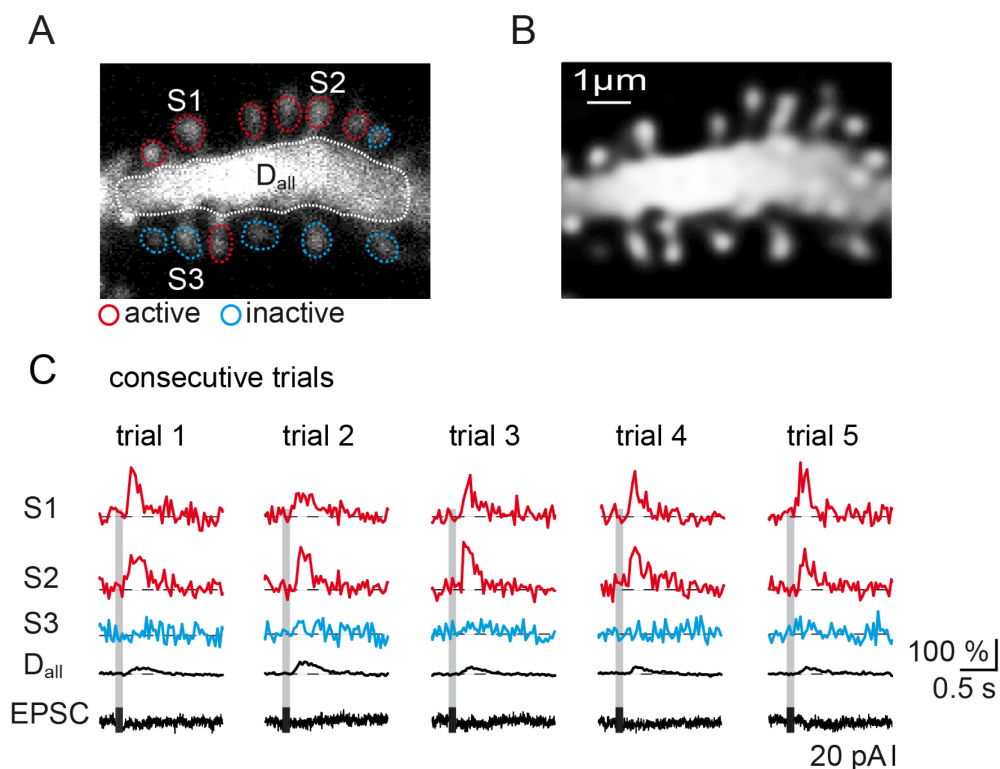


Figure 3.9: mGluR1 mediated responses in Purkinje cell spines evoked by sparse parallel fiber stimulation

(A) Average intensity projection (1280 frames at 320Hz) of the imaged spinodendritic area as acquired during one trial with sparse parallel stimulation (SPFS). Analyzed spines are denominated as active spines and encircled in red if the spine displayed at least one response after stimulation. Spines are encircled in blue if the spine showed no response during the entire experiment and are denominated as inactive spines. The analyzed dendritic area is encircled in white. **(B)** Maximum projection of two layers (1500 averaged frames / layer) of a deconvoluted z-stack recorded at the end of the experiment. **(C)** Five consecutive trials of spines numbered serially (S1-S3) in (A) and of the overall dendritic compartment (D_{all}) in addition to the associated EPSC (bottom).

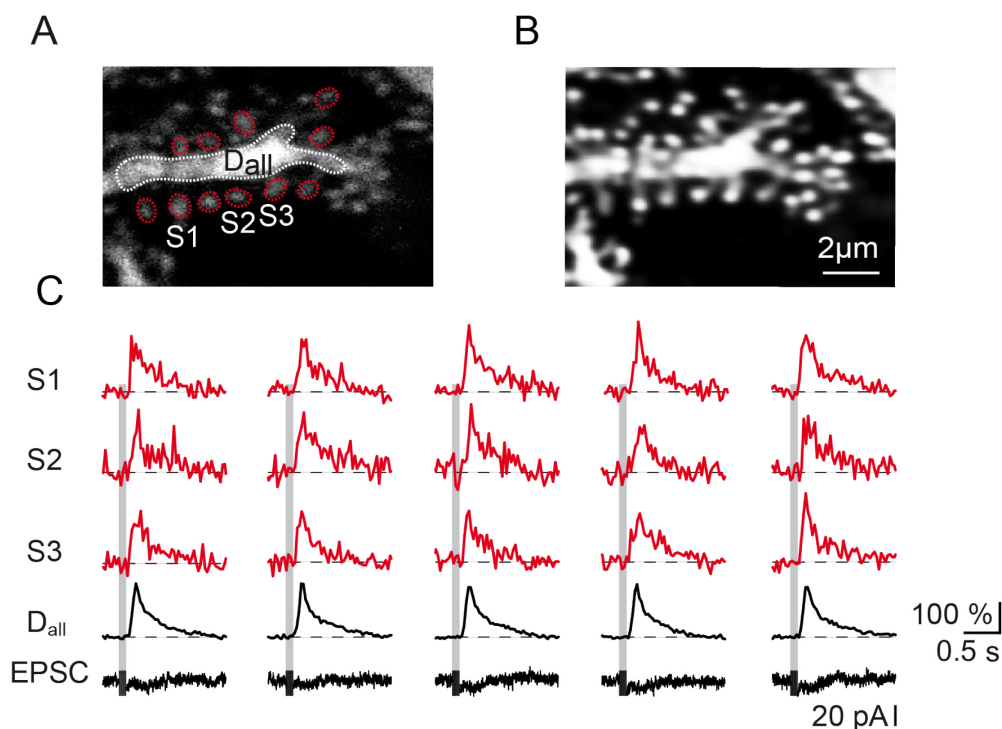


Figure 3.10: mGluR1 mediated responses in Purkinje cell spines evoked by dense parallel fiber stimulation

(A) Average intensity projection (1280 frames at 320Hz) of the imaged spinodendritic area as acquired during one trial with dense parallel stimulation (DPFS). Active spines are encircled in red and the analyzed dendritic compartment in white. (B) Maximum projection of two layers (1500 averaged frames / layer) of a deconvoluted z-stack recorded from the same area shown in (A). (C) Five consecutive trials of spines numbered serially (S1-S3) in (A) and of the overall dendritic compartment (D_{all}) in addition to the associated EPSC (bottom). With DPFS a small sEPSC is discernible.

3.8 Quantitative comparison of mGluR1-dependent spine Ca^{2+} transients evoked by sparse and dense parallel fiber stimulation

In order to quantitatively compare the Ca^{2+} transients evoked by the two different modes of stimulation, delay, rise time, amplitude and decay time constant were analyzed as schematically shown in Fig. 2.4. For all parameters analyzed the signals evoked by SPFS showed highly significant difference compared to signals evoked with DPFS (Fig. 3.11C – 3.11F). Overall these results not surprisingly

demonstrate a higher Ca^{2+} load of a spiny dendrite due to activation of many parallel fibers resulting in a longer rise time, higher amplitude and consequently in a longer decay time constant.

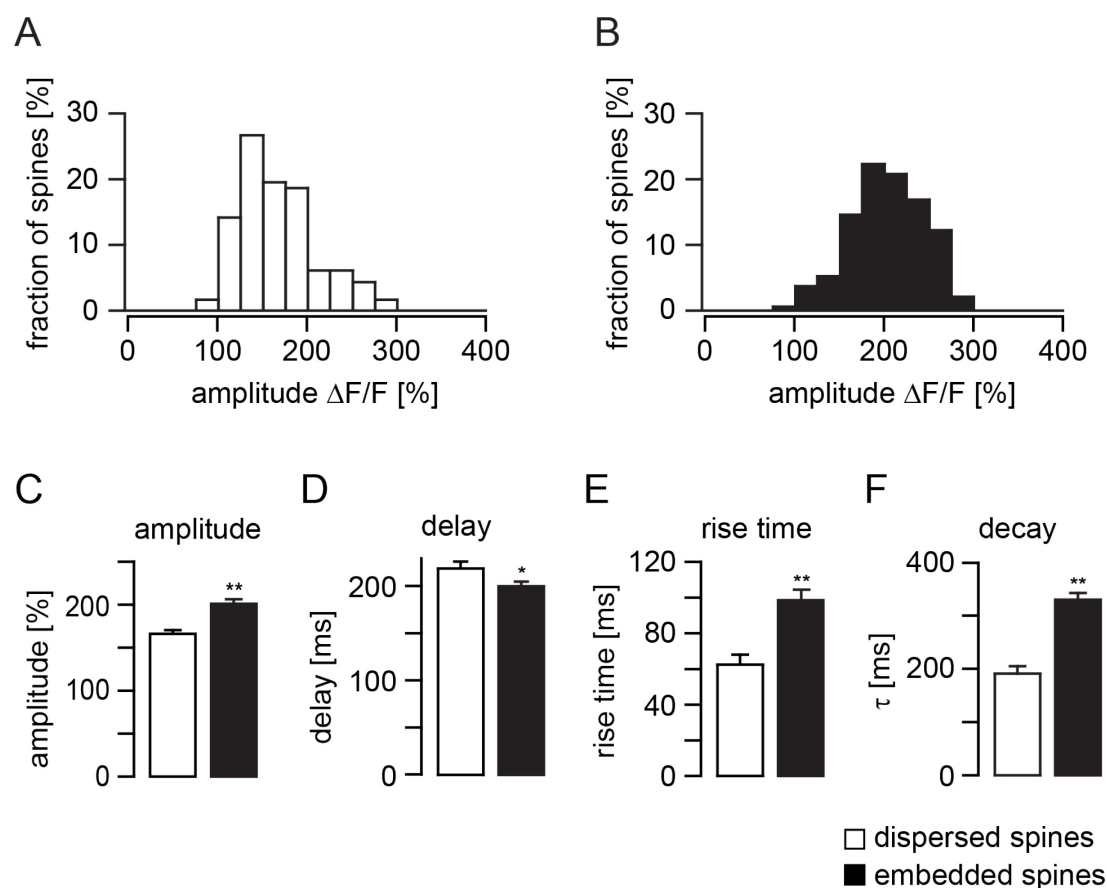


Figure 3.11: Quantitative comparison of mGluR1 mediated responses evoked by sparse and dense parallel fiber stimulation

(A) Amplitude histogram of spine responses evoked by sparse parallel fiber stimulation (n = 112 responses from 28 spines in 8 cells). (B) Amplitude histogram of spine responses evoked by dense parallel fiber stimulation (n = 129 responses from 31 spines in 6 cells). (C) Summary of the Ca^{2+} transient amplitude evoked by SPFS and DPFS in wild type mice (SPFS: 166.3 ± 4.1 , 112 responses from 28 spines, 8 cells; DPFS: 202.5 ± 3.8 , 129 responses from 31 spines, 6 cells; $p = 0.0001$). (D) Summary of the Ca^{2+} transient delay measured from begin of stimulation evoked by SPFS and DPFS in wild type mice (SPFS: 218.8 ± 6.2 , 112 responses from 28 spines, 8 cells; DPFS: 199.7 ± 4.3 , 129 responses from 31 spines, 6 cells, $p = 0.01$). (E) Summary of the Ca^{2+} transient rise time evoked by SPFS and DPFS in wild type mice (SPFS: 63.4 ± 4.3 , 112 responses from 28 spines, 8 cells; DPFS: 99.5 ± 4.8 , 129 responses from 31 spines, 6 cells; $p = 0.0001$). (F) Summary of the Ca^{2+} transient decay time constant evoked by SPFS and DPFS in wild type mice (SPFS: 194.3 ± 10.4 , 112 responses from 28 spines, 8 cells; DPFS: 333.6 ± 9.3 , 129 responses from 31 spines, 6 cells, $p = 0.0001$).

3.9 Synaptically evoked TRPC3-mediated Ca^{2+} -influx in spines

With synaptic stimulation as well as local agonist application a CPA-resistant Ca^{2+} signal due to TRPC3-mediated Ca^{2+} influx downstream of mGluR1 was identified in dendrites with the use of the spinning disc confocal imaging system (see 3.5 and 3.6). The AOD-based two-photon imaging system was employed in order to determine whether this type of signal can be detected in Purkinje cell spines, too. Again, parallel fibers were repetitively stimulated (10x with 100Hz) in the presence of a high CNQX concentration (40 μM) and OGB-1 fluorescence response was recorded in spiny dendrites using the AOD-based two-photon imaging system. Fig. 3.12 and Fig. 3.13 demonstrate the results of these experiments. Dense parallel fiber stimulation of the dendritic region presented in Fig. 3.12A was followed by the mGluR1-dependent sEPSC and Ca^{2+} transient (Fig. 3.12B left, lower and upper trace). Application of CPA (30 μM) to the external solution left the sEPSC unaffected (Fig. 3.12B right lower trace) but revealed the CPA resistant Ca^{2+} component (Fig. 3.12B right upper trace and 3.12E). This small and slow Ca^{2+} component was also discovered in dendritic spines (Fig. 3.12D). The amplitude of the CPA-resistant Ca^{2+} signal on average equals only 8.8% of the total mGluR1-mediated compound Ca^{2+} transient. The somatically recorded sEPSC that follows dense parallel fiber stimulation is not affected by the presence of CPA.

In the analogous experiment performed in TRPC3-deficient mice, the mGluR1 dependent Ca^{2+} transient could be evoked by dense parallel fiber synaptic stimulation (10x at 100Hz) without the associated inward current (Fig. 3.13B left traces). After depletion of internal stores with CPA (30 μM) the mGluR1 dependent Ca^{2+} signal was completely abolished (Fig. 3.13B right traces) and in none of the analyzed dendritic spines, a CPA resistant Ca^{2+} transient could be detected (Fig. 3.13D and 3.13E), demonstrating once again that the Ca^{2+} transient, recorded in control conditions in TRPC3-deficient mice, is a pure release signal from intracellular Ca^{2+} stores.

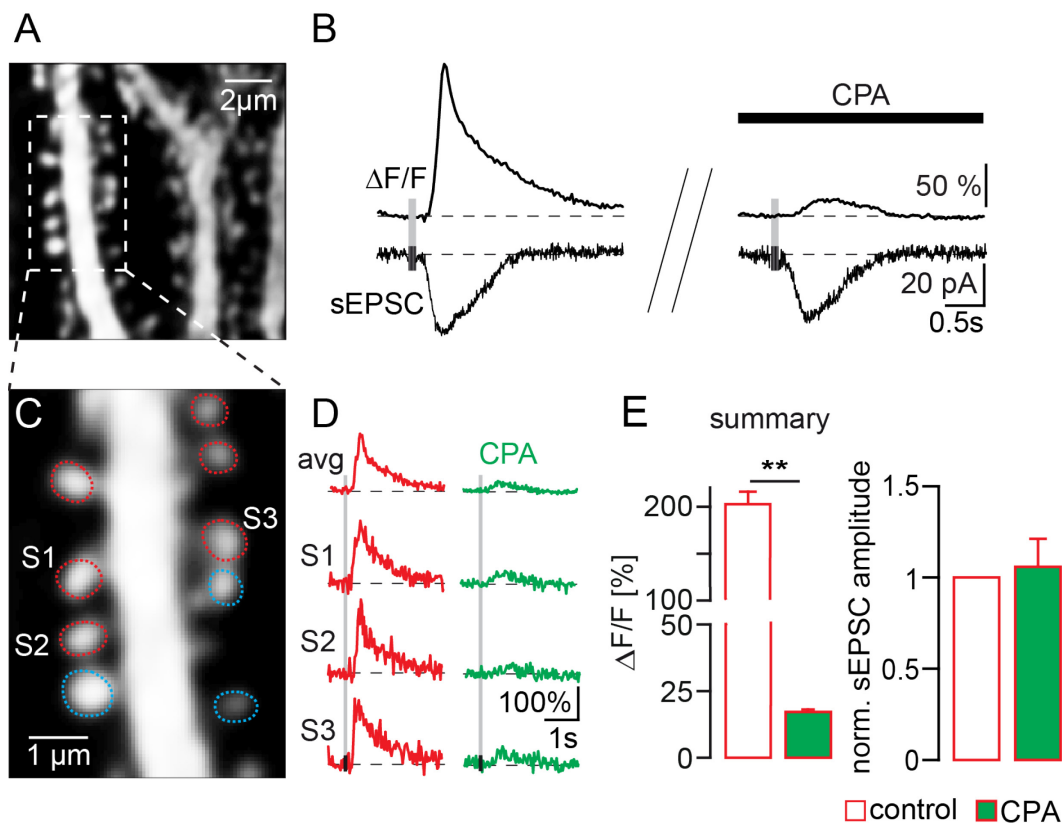


Figure 3.12: Recording of the TRPC3 mediated Ca^{2+} component in Purkinje cell spines

(A) Two-photon image of the recorded dendritic region (z-projection of 1500 images). The inset enclosed by the dashed line is shown with greater magnification in (C). (B) Lower traces: sEPSCs evoked by a short parallel fiber burst (10 pulses, 100 Hz, 40 μM CNQX) under control conditions (left) and in the presence of 30 μM CPA (right). Upper traces: Ca^{2+} transients recorded in parallel with the sEPSCs in the whole dendritic region. (C) Two-photon image of the dendritic branchlets with spines from the inset in (A). Spines are encircled in red in case of a discernible signal after CPA application or in blue if no discernible CPA-resistant signal was present. Traces of spines labeled S1-S3 are shown in (D). (D) Spine Ca^{2+} transients evoked under control conditions (red traces) and in the presence of 30 μM CPA (green traces). Traces are averages of two consecutive trials. On top the average signal of all spines which displayed a CPA resistant signal is shown. (E) Summary of the spine Ca^{2+} measurements (left) and sEPSC (right) under control conditions and in the presence of 30 μM CPA. Bar graphs show mean amplitudes of relative fluorescence changes ($\Delta F/F$) and the normalized sEPSC amplitude to control condition. Asterisks denote statistical significance ($p = 0.0001$ – highly statistical difference).

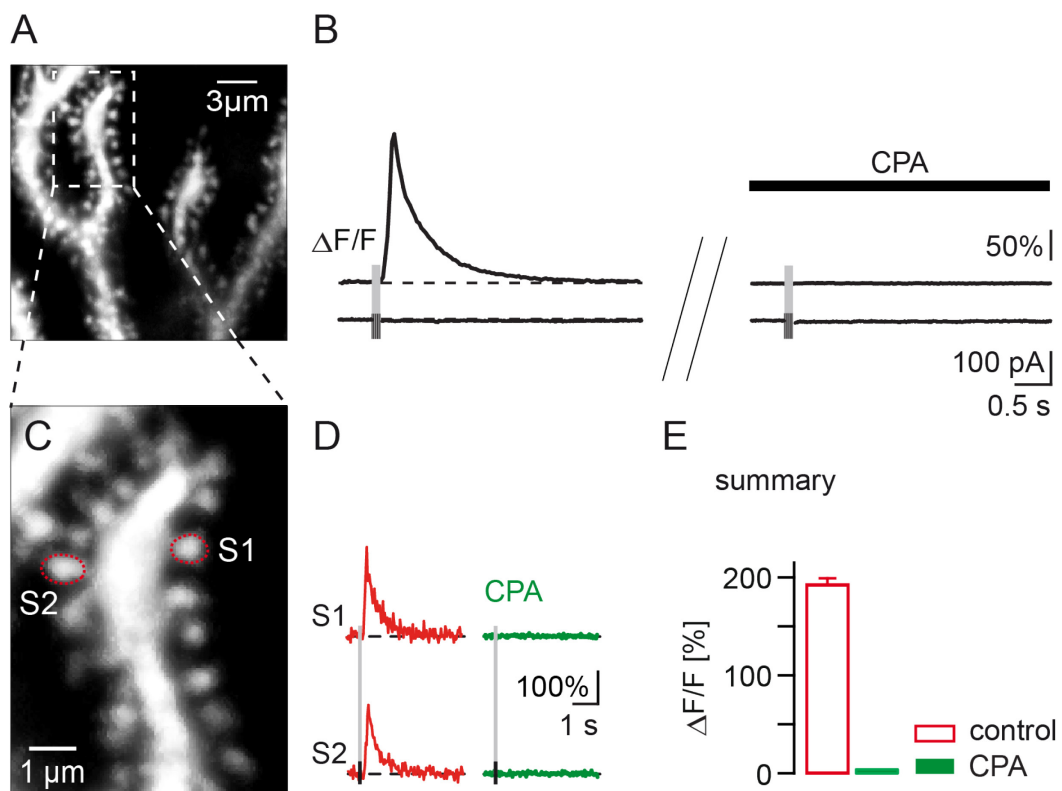


Figure 3.13: TRPC3 mediated Ca^{2+} component is absent in TRPC3-deficient mice

(A) Two-photon image of spiny dendritic branchlets from a TRPC3-deficient mouse (z-projection of 1500 frames). The inset enclosed by the dashed line is shown with greater magnification in (C). (B) Upper traces: Ca^{2+} transient in response to the synaptic stimulation in control conditions (left) and in the presence of 30 μM CPA (right). The lower traces show the simultaneously recorded whole-cell voltage clamp measurement. (C) Inset from (A) with greater magnification. Traces from spines labeled S1 and S2 are displayed in (D). (D) Ca^{2+} transients from the indicated spines during the same recordings as (B). Measurements under control conditions (red traces) and in the presence of CPA (green traces). (E) Summary of the experiments with synaptic stimulation. Bargraphs represent mean amplitudes of relative fluorescence changes ($\Delta F/F$).

3.10 Synaptically evoked mGluR1-mediated Ca^{2+} -release in spines

With sparse and dense parallel fiber stimulation the mGluR1-dependent Ca^{2+} -signals in Purkinje cell spines in TRPC3-deficient mice were evoked analogously to the wild type. Without the contribution of TRPC3-mediated Ca^{2+} -influx these transients are „pure“ Ca^{2+} -release signals.

For spine imaging whole-cell patch-clamped Purkinje cells were filled with 100 μM OGB-1. The SPFS and DPFS were applied as described in section 3.7. Following sparse parallel fiber stimulation, mGluR1-dependent Ca^{2+} transients in single, dispersed spines could be repeatedly evoked in spines without a corresponding signal in neighboring spines (Fig. 3.14A and 3.14B).

In contrast to SPFS, the Ca^{2+} -transients evoked with DPFS could be detected in all spines analyzed during the whole course of the experiment (Fig. 3.14C and 3.14D).

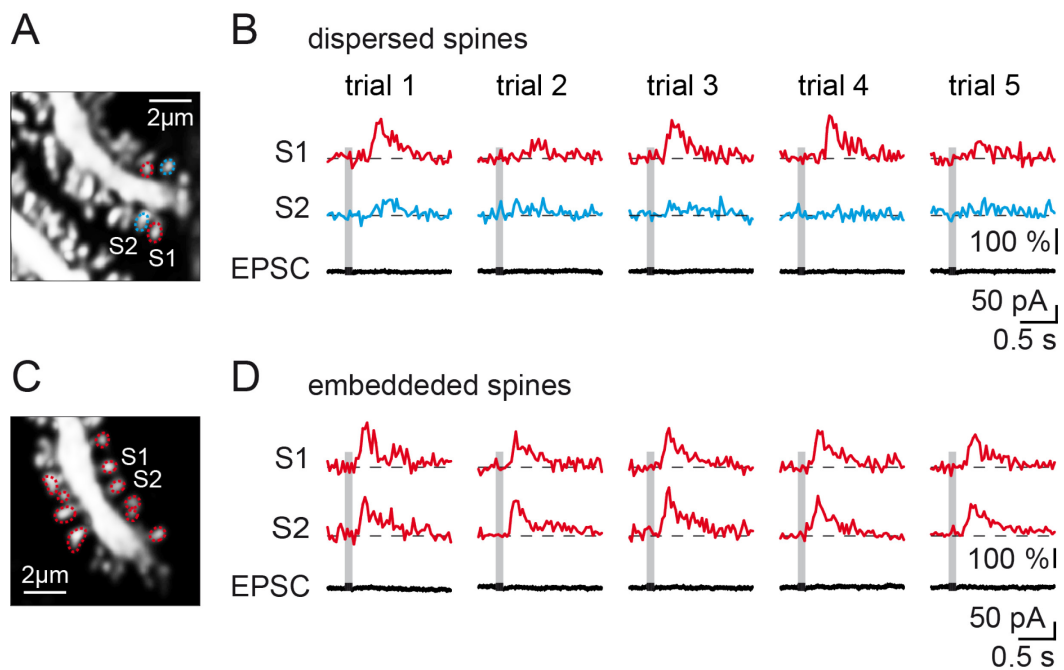


Figure 3.14: mGluR1 dependent spine Ca^{2+} signaling in TRPC3-deficient mice

(A) Two-photon image of spines on a dendritic branchlet of a whole-cell patch-clamped Purkinje cell filled with Oregon Green BAPTA-1 in a TRPC3-deficient mouse (z-projection 1500 frames). Red circles denotes active spines, blue circles denotes inactive spines (see Fig. 3.9). **(B)** Top traces: Ca^{2+} transients obtained from the labeled spines (S1 and S2) following consecutive trials evoked with SPFS. Bottom traces: Whole-cell voltage clamp recordings from the soma. **(C)** Two-photon image analogous to the one shown in (A). **(D)** Ca^{2+} traces (top traces) from indicated spines in (C) and EPSC (bottom traces) recordings evoked with DPFS.

3.11 Contribution of TRPC3 to mGluR1-mediated spine Ca^{2+} signaling

In order to determine a possible contribution of TRPC3-mediated Ca^{2+} influx to mGluR1-mediated synaptic spine Ca^{2+} signaling, spine signals in the wild type and the TRPC3-deficient mice were quantitatively compared. Again, in TRPC3-deficient mice, the time constants of decay, the amplitudes, delay and rise times were determined for Ca^{2+} transients evoked with SPFS (Fig. 3.14A and 3.14B) and with DPFS (Fig. 3.14C and 3.14D) as indicated in Fig 2.4. These parameters were compared to those obtained in wild type mice (Fig. 3.11). Bar graphs in Fig. 3.15 summarize the results of this comparison.

The amplitude in TRPC3 $-/-$ sparsely activated spines was significantly lower compared to the signal recorded in wild type mice (wild type: 166.3 ± 4.1 , 112 responses from 28 spines, 8 cells; TRPC3 $-/-$: 149.4 ± 4.9 , 102 responses from 49 spines, 9 cells, $p = 0.01$) and the signal delay was highly significant longer in TRPC3 $-/-$ mice compared with wild type mice (wild type: 218.8 ± 6.2 , 112 responses from 28 spines, 8 cells; TRPC3 $-/-$: 265.5 ± 8.6 , 102 responses in 49 spines, 9 cells, $p = 0.0001$). These results indicate that the contribution of TRPC3-dependent Ca^{2+} influx to overall mGluR1 mediated Ca^{2+} signaling in Purkinje cells spines is rather small. In conclusion, this result shows that mGluR1-mediated Ca^{2+} signaling is clearly dominated by Ca^{2+} release from intracellular stores.

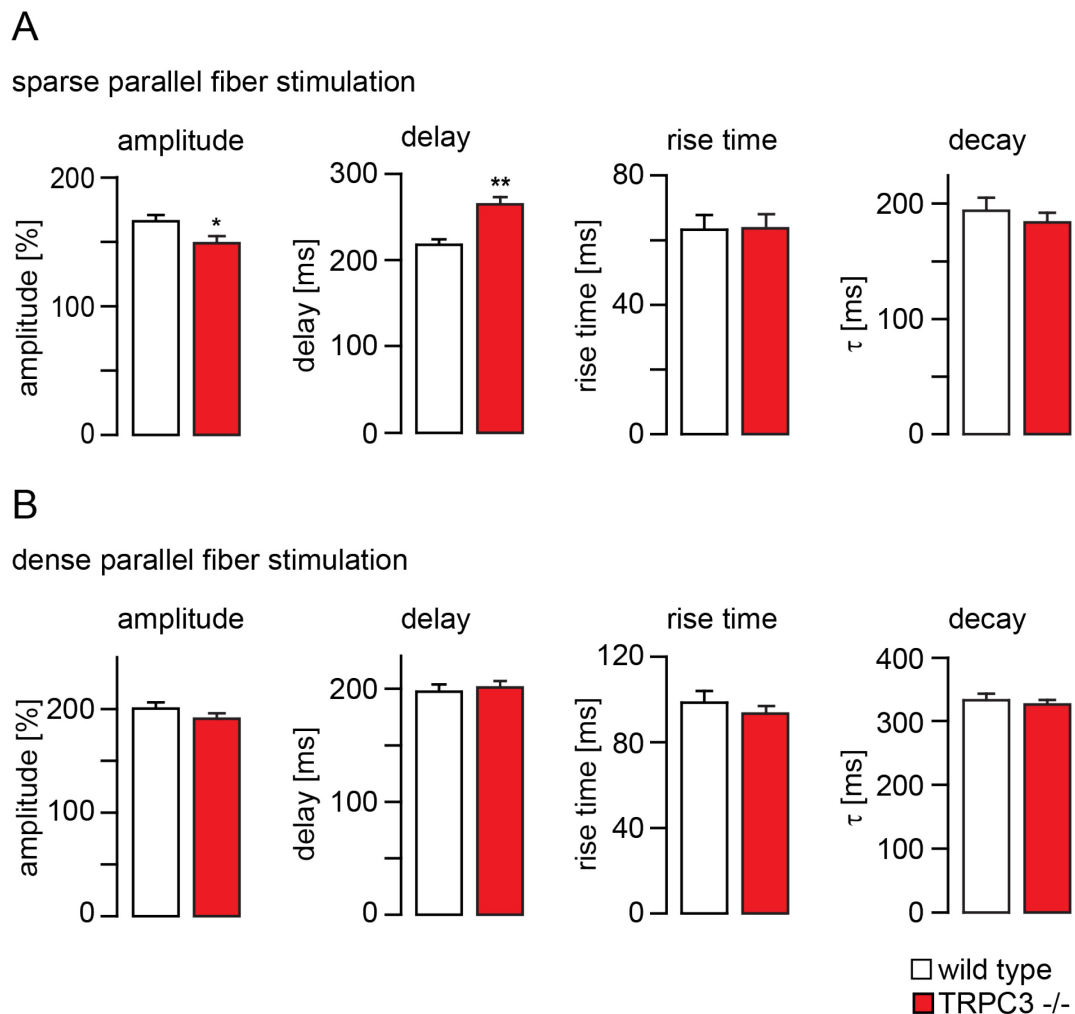


Figure 3.15: Contribution of TRPC3- mediated Ca^{2+} influx to mGluR1-dependent spine Ca^{2+} signaling

(A) Summary of the spine Ca^{2+} measurements in wild type (white bars) and TRPC3-deficient mice (red bars) evoked by SPFS. From left to right: mean values for amplitude, delay, rise time and decay time constant as exemplified in Fig. 2.4 **(B)** Analogous summary of the spine Ca^{2+} measurements in wild type (white bars) and TRPC3-deficient mice (red bars) evoked by DPFS. (* - stat. sig., $p < 0.01$; ** - highly stat. diff., $p=0.001$).

3.12 TRPC3 is not involved in LTD induction

Integrity of the mGluR1-dependent signaling cascade is a prerequisite for the induction of long-term depression (LTD) at parallel fiber-Purkinje cell synapses (Aiba et al., 1994; Hartmann et al., 2004; Ichise et al., 2000; Miyata et al., 2001). This type of synaptic plasticity has been implicated in motor learning, one of the major functions of the cerebellum (Ito, 2000). It has been shown that LTD depends on release of Ca^{2+} from internal stores downstream of mGluR1 in Purkinje cell spines (Miyata et al., 2000). In order to elucidate a possible role of TRPC3 in LTD induction, LTD at parallel fiber-Purkinje cell synapses was tested in cerebellar slices from TRPC3-deficient and wild type mice. After the whole-cell configuration was achieved the stimulating electrode was placed in the molecular layer near the soma of the patch-clamped Purkinje cell and the parallel fiber input to be tested was identified by characteristic features of parallel fiber-evoked EPSCs (graded response, paired-pulse facilitation; (Konnerth et al., 1990)). A second stimulating electrode connected to its own isolated pulse stimulator was placed in the granular layer beneath the soma of the patch-clamped Purkinje cell and EPSCs evoked by the climbing fiber that innervates the cell were identified by their all-or-none character and paired-pulse depression (Konnerth et al., 1990). The protocol used for LTD induction comprised pairing of parallel and climbing fiber stimulation for 5 min at 0.33 Hz with action potential firing due to superthreshold depolarization of the Purkinje cell. The parallel fiber-evoked AMPA receptor-mediated EPSC was activated by single-shock stimulation and monitored 5 minutes before and 45 minutes after the induction protocol was applied (Fig. 3.16A and 3.16B). In the wild type mice the amplitude of the EPSC was reduced on average by 37% (n=5) after LTD induction and this reduction lasted for the duration of the experiment (at least 45 min). The same observation was made in the absence of TRPC3 in the majority of cells tested. On average, LTD in TRPC3 $-/-$ mice is slightly reduced compared to the wild type but this difference is not significant (p= 0.15; Fig. 3.16C). Thus TRPC3 is not essentially required for LTD induction in Purkinje cells.

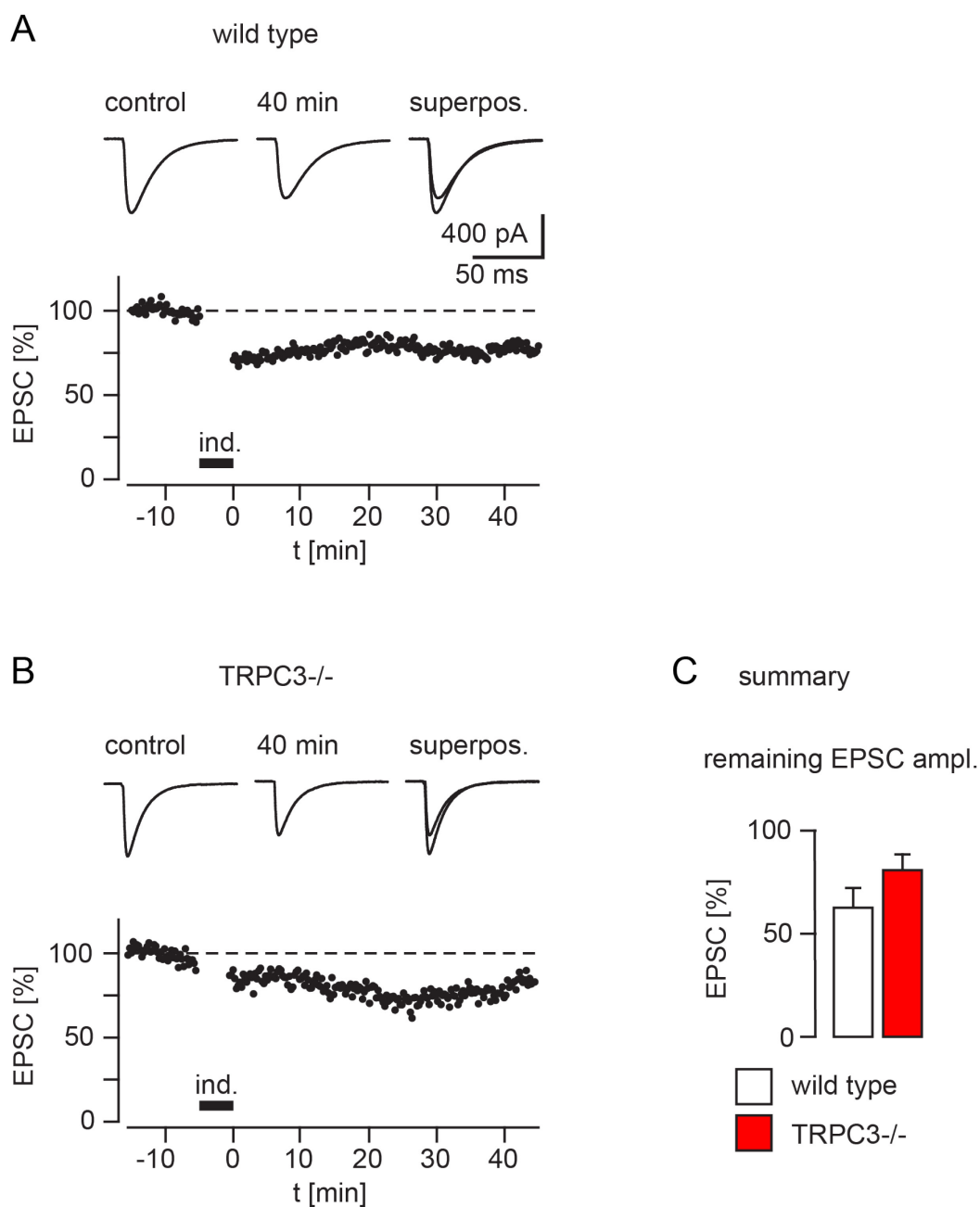


Figure 3.16: Role of TRPC3 in LTD induction

(A) Top: Single shock-evoked EPSCs (mean of ten consecutive traces) before and 40 minutes after induction of LTD. Superimposed traces on the right. Bottom: Time course of EPSC amplitudes normalized to the baseline before and after induction of LTD. Application of the LTD induction protocol (combined parallel fiber and climbing fiber activation in parallel to depolarization of the cell to threshold for 350ms with a frequency of 0.33Hz for 5 minutes) is indicated with a black bar. **(B)** Analogous experiment as shown in (A), in a TRPC3 deficient mouse. **(C)** Summary of the responses recorded after 40 minutes after LTD induction in wild type mice (white bars, $n = 5$ cells) and TRPC3 ^{-/-} mice (red bars, $n = 5$ cells).

3.13 Synaptically evoked mGluR1-dependent Ca^{2+} release is robust in the absence of TRPC3

Because TRPC subunits form Ca^{2+} -permeable channels that are activated downstream of PLC-coupled receptors (Villereal, 2006) they have been implicated in Ca^{2+} store refilling (Worley et al., 2007).

The experiment shown in Fig. 3.17 was designed to test this hypothesis for TRPC3 in Purkinje cells. Purkinje cells were whole-cell patch-clamped in sagittal cerebellar slices from wild type and TRPC3-deficient mice and filled with 100 μM OGB-1 through the patch pipette. Parallel fibers were stimulated with a burst of stimuli (10 stimuli at 100Hz in the presence of 40 μM CNQX) every two minutes for ten times and OGB-1 fluorescence change resulting from the mGluR1-dependent Ca^{2+} rise was recorded with confocal imaging (Fig. 3.17A). Both in the wild type and in the TRPC3-deficient mice there was no noticeable rundown of the Ca^{2+} response for ten stimulations (Fig 3.17). Thus, Ca^{2+} content and responsiveness of Purkinje cell ER Ca^{2+} stores are intact in the absence of TRPC3.

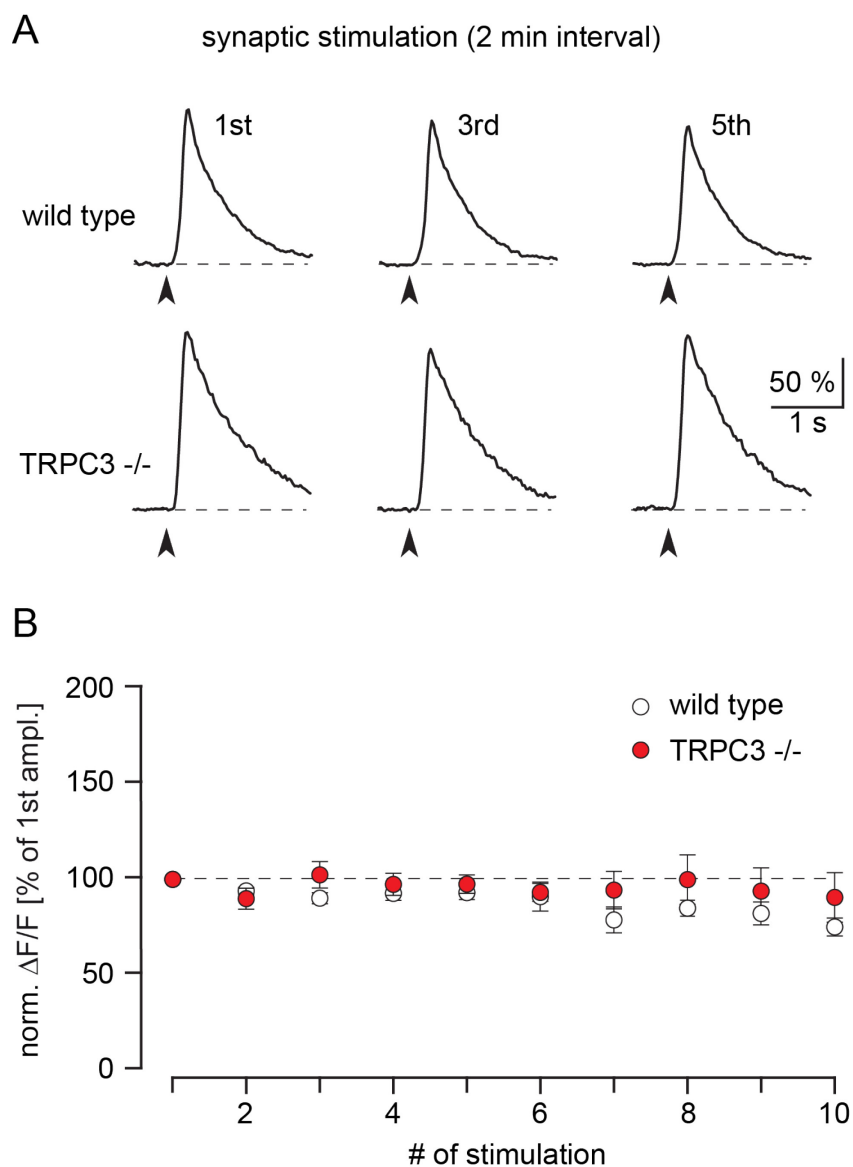


Figure 3.17: Role of TRPC3 in store refilling

(A) Ca²⁺ transients evoked in Purkinje cell dendrites of wild type mice (top traces) and TRPC3^{-/-} mice (bottom traces) with consecutive synaptic stimulation (10 stimuli at 100Hz) with 2 minutes intervals between the stimulations. **(B)** Mean amplitudes of Ca²⁺ traces for ten consecutive stimulations in wild type mice (white dots, n = 4 cells) and TRPC3^{-/-} mice (red dots, n = 6 cells).

4 Discussion

The results from the study presented here demonstrate that TRPC3 is crucial for slow mGluR1-mediated synaptic transmission in cerebellar Purkinje cells. In contrast to earlier suggestions (Kim et al. 2003) TRPC1 is not required for mGluR1-mediated signaling in Purkinje cells. Ca^{2+} imaging experiments performed in this study in wild type and TRPC3-deficient mice revealed that mGluR1-dependent synaptic Ca^{2+} transients are the sum of two types of signals: InsP_3 receptor-dependent release of Ca^{2+} ions from ER Ca^{2+} stores and Ca^{2+} influx through TRPC3 with Ca^{2+} release being the dominating component.

In summary, work presented in the thesis shows that TRPC3 in cerebellar Purkinje cells is a novel postsynaptic channel that is located and synaptically activated in spines where it contributes to postsynaptic Ca^{2+} signaling. Furthermore, two distinct mGluR1-dependent Ca^{2+} signals can be found in Purkinje cell spines: InsP_3 receptor-mediated Ca^{2+} release from stores and TRPC3-mediated Ca^{2+} influx.

On the basis of these and earlier results slow mGluR1-dependent synaptic transmission at parallel fiber synapses of Purkinje cells can be described by the model depicted in Fig. 4.1.

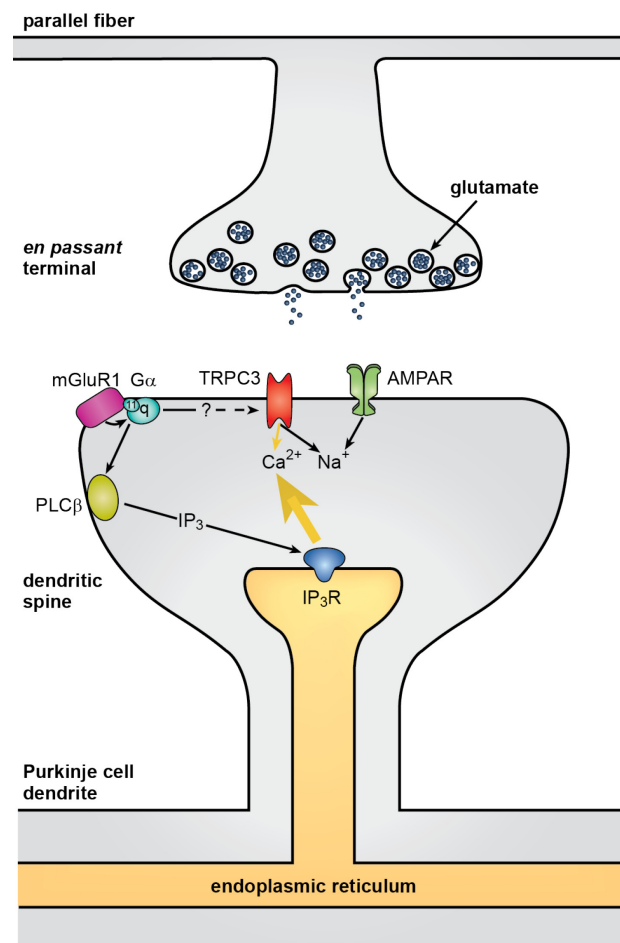


Figure 4.1: : Glutamatergic synaptic transmission at parallel fiber synapses

Glutamate released from parallel fiber presynaptic terminals binds to AMPA receptors and the mGluR1. Na $^+$ influx through AMPA receptor channels depolarizes the postsynaptic membrane. This opens voltage-gated Ca $^{2+}$ channels (not shown; Eilers et al., 1995). Binding of glutamate to the mGluR1 activates two different pathways, predominantly by G α_q with a little contribution of G α_{11} (Hartmann et al., 2004). MGLuR1 is coupled to the PLC β . One of the products of the PLC β , InsP $_3$, releases Ca $^{2+}$ ions from ER Ca $^{2+}$ stores through InsP $_3$ receptors. Through Gq proteins (Hartmann et al., 2004) and additional unresolved mechanisms of activation mGluR1 opens TRPC3. Na $^+$ and Ca $^{2+}$ influx through TRPC3 generates the sEPSC. Dissection of the compound mGluR1 mediated Ca $^{2+}$ signal revealed a large InsP $_3$ receptor mediated Ca $^{2+}$ release component and a small TRPC3 dependent Ca $^{2+}$ influx component.

In contrast to TRPC3^{-/-} mice where the sEPSC is totally absent, in mice lacking TRPC1 the sEPSC is unaffected. Considering the close interaction between mGluR1 and TRPC1 (Kim et al., 2003) and the fact that TRPC1 is expressed in Purkinje cells (Dragicevic, 2008) this was an unexpected finding. Kim et al. performed their experiments on cerebellar tissue from young rats while for the current thesis cerebellar slices from adult mice were used. Interestingly, the expression of TRPC3 in Purkinje cells is upregulated during development and is maximal in adulthood (Huang et al., 2007). Other TRPC channels are highly expressed around birth and are downregulated at later stages (Li et al., 1999). An involvement of TRPC1 in mGluR1-mediated signaling at early postnatal stages is possible. It cannot be excluded either that the species used for experiments plays a role. In addition, Kim et al., used cultured slices in contrast to acute slices that were used in the present study.

So far, TRPC channels in the brain have been implicated in developmental processes, such as cell survival, proliferation and differentiation, growth cone guidance and spine formation (Amaral and Pozzo-Miller, 2007; Jia et al., 2007; Li et al., 1999; Li et al., 2005; Tai et al., 2009). The data presented here demonstrate for the first time a direct involvement of a TRPC subunit in synaptic transmission (Hartmann et al., 2008). More recently, this was demonstrated also with the use of *moonwalker* mice that carry a spontaneous point mutation in the *TRPC3* gene. A single amino acid exchange in the sequence coding for TRPC3 leads to a gain-of-function mutation of the protein and strongly increased DHPG-evoked currents in Purkinje cells (Becker et al., 2009).

Now similar evidence is accumulating also for TRPC channels in other brain areas. Recently it has been demonstrated that TRPC channels mediate an excitatory synaptic response to glutamate in neurons of the amygdala (Faber et al., 2006). In particular TRPC5, by mediating an mGluR-dependent EPSP, has an essential role in amygdala function and fear-related behaviors (Riccio et al., 2009).

The association between the mGluR1-dependent sEPSC and influx of both Na⁺ and Ca²⁺ ions into Purkinje cell dendrites was demonstrated before (Canepari et al., 2004; Canepari and Ogden, 2006; Knöpfel et al., 2000; Linden et al., 1994; Tempia et al., 2001). With local DHPG-application, the TRPC3-mediated dendritic Ca²⁺ signal compared to the entire mGluR1-dependent Ca²⁺ transients was approximately one third in amplitude and displayed dramatically different kinetics, resembling the time course of the inward current. This result is contradictory to previously reported observations in which depletion of internal stores with CPA had

only a minor effect on the Ca^{2+} transient evoked by DHPG (Tempia et al., 2001). In those experiments, however, CPA was present in the external medium only for seven minutes, a time interval that is possibly too short for a complete depletion of stores.

In an earlier report, uncaging of glutamate over the entire dendritic tree of Purkinje cells in cerebellar slices revealed a slow and small Ca^{2+} transient measured in a small dendritic subregion. This signal was associated with the mGluR1-mediated inward current but not with Ca^{2+} release from stores. It displayed similar kinetics as the inward current and was much smaller than the overall mGluR1 mediated Ca^{2+} signal, too (Canepari and Ogden, 2006).

The study presented here, however, provides the first quantitative assessment of the contribution of Ca^{2+} entry via TRPC3 to the overall mGluR1- dependent Ca^{2+} signal in Purkinje cell spines.

Imaging with a two photon imaging system allowed direct comparison of the two mGluR1-dependent signaling components in spines, the subcellular compartments, in which the signal is generated (see Fig. 3.9). The amplitude of the Ca^{2+} transient resulting from TRPC3-mediated Ca^{2+} influx was ~8,8% of the overall mGluR1 mediated Ca^{2+} signal, indicating a small contribution of Ca^{2+} influx under physiological conditions. In accordance with that, mGluR1-dependent Ca^{2+} transients in spines of Purkinje cell in TRPC3-deficient mice differed little from the ones recorded in wild type mice (Fig. 3.15). The recording of Ca^{2+} release in single spines in the TRPC3-deficient mice shows that the Ca^{2+} release machinery in single spines is functional without TRPC3.

In heterologous expression systems TRPC3 has been described as a highly Ca^{2+} -permeable channel (Zitt et al., 1997) with a $\text{Ca}^{2+}/\text{Na}^+$ ratio of 1.6 (Gees et al., 2010; Venkatachalam and Montell, 2007). Hence, the question arises why the signal measured here is so small? One likely possibility is that the channel expressed at Purkinje cell synapses is composed not only of TRPC3 but also of other subunits. It has been demonstrated that the subunit composition strongly affects properties of TRPC channels (Lintschinger et al., 2000). In line with that the IV-curve of the mGluR1 dependent inward current in Purkinje cells strongly differs from that of “pure” TRPC3 channels (Hartmann, personal communication). In addition, the conditions in the “perisynaptic signaling complex” at parallel fiber synapse could also influence channel properties. A direct functional interaction of TRPC3 with the scaffolding protein Homer and InsP_3 receptors has been demonstrated (Kim et al., 2006; Kiselyov et al., 1998). It is also known that mGluR1, InsP_3 receptors and

Homer1 are assembled in signaling complexes in Purkinje cells synapses (Nakamura et al., 2004). Thus, it can be speculated that TRPC3 as part of the signaling complex in Purkinje cell spines possesses different properties as observed in heterologous systems. In HEK-293 and COS7 cells TRPC channels have been shown to directly associate with Orai proteins (Liao et al., 2007). Orai1-3 are expressed in Purkinje cells (Karl and Hartmann, personal communications) and a possible interaction between TRPC3 and Orai channels must be considered for Purkinje cells, too.

One of the questions that was pursued in this work is that about the function of TRPC3 for Purkinje cell physiology. Purkinje cells provide the sole output of the cerebellar cortex and are therefore essential for cerebellar function like motor control and motor learning.

Behavioral tests showed significant impairment of motor control for TRPC3-deficient mice compared to wild type mice (Hartmann et al., 2008). TRPC3 is widely expressed throughout the brain including brain areas that are involved in motor functions like the basal ganglia (Berg et al., 2007; Zhou et al., 2008). There TRPC3 is also deleted in the general knockout used for the present study. However, the expression of TRPC3 in Purkinje cells is much higher than anywhere else in the brain (Lein et al., 2007). In addition, the motor phenotype of the TRPC3-deficient mice closely resembles that of Purkinje cell type calbindin D28k-deficient mice (Barski et al., 2003). Thus, the reduced motor control in the TRPC3-deficient mice can be largely attributed to cerebellar dysfunction. Similarly, although *moonwalker* mice are characterized by a genomic mutation of *TRPC3*, heterozygous carriers exhibit severe symptoms of ataxia (Becker et al., 2009) one of the hallmarks of disturbed cerebellar function. In addition, mice with a Purkinje cell type-specific deletion of TRPC3 display behavioral deficits that are comparable to the general TRPC3 knockouts (Adelsberger, personal communication). One possibility for the cause of cerebellar dysfunction could be impaired long-term depression (LTD) due to interference with the mGluR1 pathway. This had been shown in mGluR1-deficient mice (Aiba et al., 1994; Ichise et al., 2000), in mice where either $G\alpha_q$ or $G\alpha_{11}$ protein was deleted (Hartmann et al., 2004) and in mice with a PLC β 4 deletion (Miyata et al., 2001). Additionally, in Myosin-Va deficient mice where the smooth endoplasmic reticulum is absent in Purkinje cell dendritic spines, LTD cannot be induced (Miyata et al., 2000). The TRPC3-mediated Ca^{2+} influx, although slow and small, could be an important step in this complex episode leading finally to LTD. But, based on the results gained from the LTD experiments in this study (Fig. 3.16) an essential role of

TRPC3-mediated Ca^{2+} influx signal for LTD induction could not be shown. Hence, an impaired LTD cannot explain the phenotype observed in TRPC3-deficient mice.

A role for TRPC channels in refilling of internal Ca^{2+} stores after depletion downstream of metabotropic receptor activation has been suggested (Worley et al., 2007). But different lines of evidence speak against a critical involvement of TRPC3 and hence of the sEPSC in store refilling. First, amplitudes and spatial dimensions of mGluR1-dependent dendritic Ca^{2+} transients are not affected by the absence of TRPC3. Also, these Ca^{2+} transients could be repeatedly evoked in TRPC3 $-/-$ mice without noticeable rundown for many times, similarly to wild type mice. These results indicate that impaired motor function in TRPC3-deficient mice does not occur due to disturbed refilling of internal Ca^{2+} stores.

It has been reported that mGluR1-mediated signaling influences Purkinje cell firing rates (Yamakawa and Hirano, 1999; Yuan et al., 2007). Also, in other brain systems it has been shown that TRPC channels influence neuronal firing rates (Berg et al., 2007; Cvetkovic-Lopes et al., 2010; Zhou et al., 2008). Rather than affecting LTD or Ca^{2+} store homeostasis TRPC3 therefore seems to have a direct action in Purkinje cell firing thereby shaping the output of the cerebellar cortex and hence, cerebellar function.

The molecular players leading to activation of TRPC3 at the parallel fiber to Purkinje cell synapse are largely unknown. It has been shown that activation of the sEPSC and hence TRPC3 relies primarily on activation of the $\text{G}\alpha_q$ protein (Hartmann et al., 2004). Conflicting data exist regarding the role of $\text{PLC}\beta$ in generation of the sEPSC. While in animals lacking the $\text{PLC}\beta_4$ the sEPSC was absent (Sugiyama et al., 1999), experiments, in which the $\text{PLC}\beta$ antagonist U73122 was used, demonstrated no effect on the mGluR1 dependent inward current (Canepari et al., 2004; Glitsch, 2010; Hirono et al., 1998; Tempia et al., 1998). TRPC3 together with TRPC6 and TRPC7 form the subfamily of diacylglycerol (DAG)-activated TRPC channels. DAG as the second product of the $\text{PLC}\beta$ could possibly contribute to TRPC3 activation in Purkinje cells. A recent publication showed that the Phospholipase D1 could be involved in the process of sEPSC activation (Glitsch, 2010). Furthermore, activation of TRPC3 by the ER Ca^{2+} sensor STIM1 has been reported in HEK cells (Liao et al., 2007). STIM1 is also expressed in Purkinje cells (Karl and Hartmann, personal communications) and this could be another or an additional mechanism for TRPC3 activation. Thus, the gating mechanism(s) leading to opening of TRPC3 downstream of mGluR1 remain(s) to be elucidated.

5 Publications

Hartmann J, Dragicevic E, Adelsberger H, **Henning HA**, Sumser M, Abramowitz J, Blum R, Dietrich A, Freichel M, Flockerzi V, Birnbaumer L, Konnerth A. (2008) **TRPC3 channels are required for synaptic transmission and motor coordination** Neuron 59: 392-8

Chen X, Kovalchuk Y, Adelsberger H, **Henning HA**, Sausbier M, Wietzorrek G, Ruth P, Yarom Y, Konnerth A. (2010) **Disruption of the olivo-cerebellar circuit by Purkinje neuron-specific ablation of BK channels** Proc Natl Acad Sci U S A 107: 12323-8

Hartmann J, **Henning HA**, Konnerth A
mGluR1/TRPC3-mediated synaptic transmission and calcium signaling in mammalian central neurons (in press)

Busche MA, Chen X, **Henning HA**, Reichwald J, Staufenbiel M, Konnerth A
Acute repair of early defects in hippocampal activity in a mouse model of Alzheimer's disease (in preparation)

Grienberger C, Rochefort N, Adelsberger H, **Henning HA**, Staufenbiel M, Konnerth A
Impaired orientation-tuning of visual cortical neurons in Alzheimer's Disease (submitted)

Henning HA, Hartmann J, Leischner U, Konnerth A
mGluR1/TRPC3 mediated Ca²⁺ signaling in dendritic spines of cerebellar Purkinje cells (in preparation)

6 Acknowledgements

This work was conducted under the supervision of Prof. Dr. Arthur Konnerth and PD Dr. Jana Hartmann.

I would like to thank Prof. Dr. Arthur Konnerth for the scientific guidance and practical advices and for giving me the opportunity and encouragement to learn and use new techniques.

I wish to thank PD Dr. Jana Hartmann for her tremendous support, advice and guidance during my time as a PhD student at the Institute of Neuroscience.

I would like to thank Prof. Dr. Helmuth Adelsberger for the advices in all matters of the PhD program.

Special thanks to Ulrich Leischner for building the AOD based two photon system and giving me herewith the opportunity to observe signals in tiny spines.

I wish to thank Martin Sumser for teaching me immunohistological methods and some unknown facts about Besigheim.

I want to thank Christine Grienberger, Xiaowei Chen and Aurel Busche for their fruitful collaboration, which gave me the opportunity to improve my histological skills.

I would like to thank all other colleagues. It has been a pleasure to work with you.

Last but not least I want to thank my family, my friends and especially Julia, for the support and encouragement through all this years.

7 References

- Aiba, A., Kano, M., Chen, C., Stanton, M.E., Fox, G.D., Herrup, K., Zwingman, T.A., and Tonegawa, S. (1994). Deficient cerebellar long-term depression and impaired motor learning in mGluR1 mutant mice. *Cell* 79: 377-388.
- Amaral, M.D., and Pozzo-Miller, L. (2007). TRPC3 channels are necessary for brain-derived neurotrophic factor to activate a nonselective cationic current and to induce dendritic spine formation. *J Neurosci* 27: 5179-5189.
- Barski, J.J., Hartmann, J., Rose, C.R., Hoebeek, F., Morl, K., Noll-Hussong, M., De Zeeuw, C.I., Konnerth, A., and Meyer, M. (2003). Calbindin in cerebellar Purkinje cells is a critical determinant of the precision of motor coordination. *J Neurosci* 23: 3469-3477.
- Bastian, A.J. (1997). Mechanisms of ataxia. *Physical therapy* 77: 672-675.
- Batchelor, A.M., and Garthwaite, J. (1993). Novel synaptic potentials in cerebellar Purkinje cells: probable mediation by metabotropic glutamate receptors. *Neuropharmacology* 32: 11-20.
- Batchelor, A.M., and Garthwaite, J. (1997). Frequency detection and temporally dispersed synaptic signal association through a metabotropic glutamate receptor pathway. *Nature* 385: 74-77.
- Batchelor, A.M., Madge, D.J., and Garthwaite, J. (1994). Synaptic activation of metabotropic glutamate receptors in the parallel fibre-Purkinje cell pathway in rat cerebellar slices. *Neuroscience* 63: 911-915.
- Baude, A., Nusser, Z., Roberts, J.D., Mulvihill, E., McIlhinney, R.A., and Somogyi, P. (1993). The metabotropic glutamate receptor (mGluR1 alpha) is concentrated at perisynaptic membrane of neuronal subpopulations as detected by immunogold reaction. *Neuron* 11: 771-787.
- Becker, E.B., Oliver, P.L., Glitsch, M.D., Banks, G.T., Achilli, F., Hardy, A., Nolan, P.M., Fisher, E.M., and Davies, K.E. (2009). A point mutation in TRPC3 causes abnormal Purkinje cell development and cerebellar ataxia in moonwalker mice. *Proceedings of the National Academy of Sciences of the United States of America* 106: 6706-6711.
- Berg, A.P., Sen, N., and Bayliss, D.A. (2007). TrpC3/C7 and Slo2.1 are molecular targets for metabotropic glutamate receptor signaling in rat striatal cholinergic interneurons. *J Neurosci* 27: 8845-8856.

- Brenowitz, S.D., and Regehr, W.G. (2007). Reliability and heterogeneity of calcium signaling at single presynaptic boutons of cerebellar granule cells. *J Neurosci* 27: 7888-7898.
- Canepari, M., Auger, C., and Ogden, D. (2004). Ca²⁺ ion permeability and single-channel properties of the metabotropic slow EPSC of rat Purkinje neurons. *J Neurosci* 24: 3563-3573.
- Canepari, M., and Ogden, D. (2006). Kinetic, pharmacological and activity-dependent separation of two Ca²⁺ signalling pathways mediated by type 1 metabotropic glutamate receptors in rat Purkinje neurones. *The Journal of physiology* 573: 65-82.
- Canepari, M., Papageorgiou, G., Corrie, J.E., Watkins, C., and Ogden, D. (2001). The conductance underlying the parallel fibre slow EPSP in rat cerebellar Purkinje neurones studied with photolytic release of L-glutamate. *The Journal of physiology* 533: 765-772.
- Chadderton, P., Margrie, T.W., and Hausser, M. (2004). Integration of quanta in cerebellar granule cells during sensory processing. *Nature* 428: 856-860.
- Clapham, D.E. (2003). TRP channels as cellular sensors. *Nature* 426: 517-524.
- Clapham, D.E., Runnels, L.W., and Strubing, C. (2001). The TRP ion channel family. *Nature reviews* 2: 387-396.
- Coesmans, M., Smitt, P.A., Linden, D.J., Shigemoto, R., Hirano, T., Yamakawa, Y., van Alphen, A.M., Luo, C., van der Geest, J.N., Kros, J.M., *et al.* (2003). Mechanisms underlying cerebellar motor deficits due to mGluR1-autoantibodies. *Annals of neurology* 53: 325-336.
- Curtis, D.R., Phillis, J.W., and Watkins, J.C. (1960). The chemical excitation of spinal neurones by certain acidic amino acids. *The Journal of physiology* 150: 656-682.
- Cvetkovic-Lopes, V., Eggermann, E., Uschakov, A., Grivel, J., Bayer, L., Jones, B.E., Serafin, M., and Muhlethaler, M. (2010). Rat hypocretin/orexin neurons are maintained in a depolarized state by TRPC channels. *PloS one* 5: e15673.
- Dietrich, A., Kalwa, H., Storch, U., Mederos, Y.S.M., Salanova, B., Pinkenburg, O., Dubrovskaja, G., Essin, K., Gollasch, M., Birnbaumer, L., and Gudermann, T. (2007). Pressure-induced and store-operated cation influx in vascular smooth muscle cells is independent of TRPC1. *Pflugers Arch* 455: 465-477.

- Dingledine, R., Borges, K., Bowie, D., and Traynelis, S.F. (1999). The glutamate receptor ion channels. *Pharmacological reviews* 51: 7-61.
- Dragicevic, E. (2008). Quantitative single-cell RT-PCR analysis of the TRPC channel subunits expression patterns in cerebellar Purkinje neurons. In Institute of Neuroscience, Faculty of Medicine (Munich, TU München), p. 92.
- Duenas, A.M., Goold, R., and Giunti, P. (2006). Molecular pathogenesis of spinocerebellar ataxias. *Brain* 129: 1357-1370.
- Eccles, J.C. (1967). Circuits in the cerebellar control of movement. *Proceedings of the National Academy of Sciences of the United States of America* 58: 336-343.
- Edwards, F.A., Konnerth, A., Sakmann, B., and Takahashi, T. (1989). A thin slice preparation for patch clamp recordings from neurones of the mammalian central nervous system. *Pflugers Arch* 414: 600-612.
- Eilers, J., Augustine, G.J., and Konnerth, A. (1995). Subthreshold synaptic Ca²⁺ signalling in fine dendrites and spines of cerebellar Purkinje neurons. *Nature* 373: 155-158.
- Faber, E.S., Sedlak, P., Vidovic, M., and Sah, P. (2006). Synaptic activation of transient receptor potential channels by metabotropic glutamate receptors in the lateral amygdala. *Neuroscience* 137: 781-794.
- Finch, E.A., and Augustine, G.J. (1998). Local calcium signalling by inositol-1,4,5-trisphosphate in Purkinje cell dendrites. *Nature* 396: 753-756.
- Gao, W., Dunbar, R.L., Chen, G., Reinert, K.C., Oberdick, J., and Ebner, T.J. (2003). Optical imaging of long-term depression in the mouse cerebellar cortex in vivo. *J Neurosci* 23: 1859-1866.
- Garaschuk, O., Yaari, Y., and Konnerth, A. (1997). Release and sequestration of calcium by ryanodine-sensitive stores in rat hippocampal neurones. *The Journal of physiology* 502 (Pt 1): 13-30.
- Gees, M., Colsoul, B., and Nilius, B. (2010). The role of transient receptor potential cation channels in Ca²⁺ signaling. *Cold Spring Harbor perspectives in biology* 2: a003962.
- Geiger, J.R., Bischofberger, J., Vida, I., Frobe, U., Pfitzinger, S., Weber, H.J., Haverkamp, K., and Jonas, P. (2002). Patch-clamp recording in brain slices with improved slicer technology. *Pflugers Arch* 443: 491-501.
- Glitsch, M.D. (2010). Activation of native TRPC3 cation channels by phospholipase D. *Faseb J* 24: 318-325.

- Groschner, K., and Rosker, C. (2005). TRPC3: a versatile transducer molecule that serves integration and diversification of cellular signals. *Naunyn-Schmiedeberg's archives of pharmacology* 371: 251-256.
- Hartmann, J., Blum, R., Kovalchuk, Y., Adelsberger, H., Kuner, R., Durand, G.M., Miyata, M., Kano, M., Offermanns, S., and Konnerth, A. (2004). Distinct roles of Galpha(q) and Galpha11 for Purkinje cell signaling and motor behavior. *J Neurosci* 24: 5119-5130.
- Hartmann, J., Dragicevic, E., Adelsberger, H., Henning, H.A., Sumser, M., Abramowitz, J., Blum, R., Dietrich, A., Freichel, M., Flockerzi, V., et al. (2008). TRPC3 channels are required for synaptic transmission and motor coordination. *Neuron* 59: 392-398.
- Haugland, R.P., Spence, M.T.Z., Johnson, I.D., and Basey, A. (2005). The handbook: a guide to fluorescent probes and labeling technologies., 10th edn (Eugene, OR: Molecular Probes).
- Hayashi, T. (1952). A physiological study of epileptic seizures following cortical stimulation in animals and its application to human clinics. *The Japanese journal of physiology* 3: 46-64.
- Hirono, M., Konishi, S., and Yoshioka, T. (1998). Phospholipase C-independent group I metabotropic glutamate receptor-mediated inward current in mouse purkinje cells. *Biochemical and biophysical research communications* 251: 753-758.
- Houamed, K.M., Kuijper, J.L., Gilbert, T.L., Haldeman, B.A., O'Hara, P.J., Mulvihill, E.R., Almers, W., and Hagen, F.S. (1991). Cloning, expression, and gene structure of a G protein-coupled glutamate receptor from rat brain. *Science* 252: 1318-1321.
- Huang, W.C., Young, J.S., and Glitsch, M.D. (2007). Changes in TRPC channel expression during postnatal development of cerebellar neurons. *Cell Calcium* 42: 1-10.
- Ichise, T., Kano, M., Hashimoto, K., Yanagihara, D., Nakao, K., Shigemoto, R., Katsuki, M., and Aiba, A. (2000). mGluR1 in cerebellar Purkinje cells essential for long-term depression, synapse elimination, and motor coordination. *Science* 288: 1832-1835.
- Inoue, S., and Inoue, T. (2002). Direct-view high-speed confocal scanner: the CSU-10. *Methods in cell biology* 70: 87-127.
- Ito, M. (2000). Mechanisms of motor learning in the cerebellum. *Brain Res* 886: 237-245.

- Ito, M. (2001). Cerebellar long-term depression: characterization, signal transduction, and functional roles. *Physiological reviews* 81: 1143-1195.
- Ito, M. (2002). Historical review of the significance of the cerebellum and the role of Purkinje cells in motor learning. *Annals of the New York Academy of Sciences* 978: 273-288.
- Ito, M. (2006). Cerebellar circuitry as a neuronal machine. *Progress in neurobiology* 78: 272-303.
- Jia, Y., Zhou, J., Tai, Y., and Wang, Y. (2007). TRPC channels promote cerebellar granule neuron survival. *Nature neuroscience* 10: 559-567.
- Jörntell, H., and Ekerot, C.F. (2006). Properties of somatosensory synaptic integration in cerebellar granule cells in vivo. *J Neurosci* 26: 11786-11797.
- Kano, M., Hashimoto, K., Kurihara, H., Watanabe, M., Inoue, Y., Aiba, A., and Tonegawa, S. (1997). Persistent multiple climbing fiber innervation of cerebellar Purkinje cells in mice lacking mGluR1. *Neuron* 18: 71-79.
- Kim, J.Y., Zeng, W., Kiselyov, K., Yuan, J.P., Dehoff, M.H., Mikoshiba, K., Worley, P.F., and Muallem, S. (2006). Homer 1 mediates store- and inositol 1,4,5-trisphosphate receptor-dependent translocation and retrieval of TRPC3 to the plasma membrane. *The Journal of biological chemistry* 281: 32540-32549.
- Kim, S.J., Kim, Y.S., Yuan, J.P., Petralia, R.S., Worley, P.F., and Linden, D.J. (2003). Activation of the TRPC1 cation channel by metabotropic glutamate receptor mGluR1. *Nature* 426: 285-291.
- Kiselyov, K., Xu, X., Mozhayeva, G., Kuo, T., Pessah, I., Mignery, G., Zhu, X., Birnbaumer, L., and Muallem, S. (1998). Functional interaction between InsP3 receptors and store-operated Htrp3 channels. *Nature* 396: 478-482.
- Knöpfel, T., Anchisi, D., Alojado, M.E., Tempia, F., and Strata, P. (2000). Elevation of intradendritic sodium concentration mediated by synaptic activation of metabotropic glutamate receptors in cerebellar Purkinje cells. *The European journal of neuroscience* 12: 2199-2204.
- Konnerth, A., Llano, I., and Armstrong, C.M. (1990). Synaptic currents in cerebellar Purkinje cells. *Proceedings of the National Academy of Sciences of the United States of America* 87: 2662-2665.

- Kovalchuk, Y., Eilers, J., Lisman, J., and Konnerth, A. (2000). NMDA receptor-mediated subthreshold Ca^{2+} signals in spines of hippocampal neurons. *J Neurosci* 20: 1791-1799.
- Lein, E.S., Hawrylycz, M.J., Ao, N., Ayres, M., Bensinger, A., Bernard, A., Boe, A.F., Boguski, M.S., Brockway, K.S., Byrnes, E.J., *et al.* (2007). Genome-wide atlas of gene expression in the adult mouse brain. *Nature* 445: 168-176.
- Leischner, U. (2011). Ultra-fast two-photon microscopy for in vivo brain imaging. In Institute of Neuroscience, Faculty of Medicine (Munich, TU München), p. 94.
- Li, H.S., Xu, X.Z., and Montell, C. (1999). Activation of a TRPC3-dependent cation current through the neurotrophin BDNF. *Neuron* 24: 261-273.
- Li, Y., Jia, Y.C., Cui, K., Li, N., Zheng, Z.Y., Wang, Y.Z., and Yuan, X.B. (2005). Essential role of TRPC channels in the guidance of nerve growth cones by brain-derived neurotrophic factor. *Nature* 434: 894-898.
- Liao, Y., Erxleben, C., Yildirim, E., Abramowitz, J., Armstrong, D.L., and Birnbaumer, L. (2007). Orai proteins interact with TRPC channels and confer responsiveness to store depletion. *Proceedings of the National Academy of Sciences of the United States of America* 104: 4682-4687.
- Liman, E.R., Corey, D.P., and Dulac, C. (1999). TRP2: a candidate transduction channel for mammalian pheromone sensory signaling. *Proceedings of the National Academy of Sciences of the United States of America* 96: 5791-5796.
- Linden, D.J., Smeyne, M., and Connor, J.A. (1994). Trans-ACPD, a metabotropic receptor agonist, produces calcium mobilization and an inward current in cultured cerebellar Purkinje neurons. *Journal of neurophysiology* 71: 1992-1998.
- Lintschinger, B., Balzer-Geldsetzer, M., Baskaran, T., Graier, W.F., Romanin, C., Zhu, M.X., and Groschner, K. (2000). Coassembly of Trp1 and Trp3 proteins generates diacylglycerol- and Ca^{2+} -sensitive cation channels. *The Journal of biological chemistry* 275: 27799-27805.
- Llano, I., Marty, A., Armstrong, C.M., and Konnerth, A. (1991). Synaptic- and agonist-induced excitatory currents of Purkinje cells in rat cerebellar slices. *The Journal of physiology* 434: 183-213.
- Marcaggi, P., and Attwell, D. (2005). Endocannabinoid signaling depends on the spatial pattern of synapse activation. *Nature neuroscience* 8: 776-781.

- Masu, M., Tanabe, Y., Tsuchida, K., Shigemoto, R., and Nakanishi, S. (1991). Sequence and expression of a metabotropic glutamate receptor. *Nature* 349: 760-765.
- Masugi-Tokita, M., Tarusawa, E., Watanabe, M., Molnar, E., Fujimoto, K., and Shigemoto, R. (2007). Number and density of AMPA receptors in individual synapses in the rat cerebellum as revealed by SDS-digested freeze-fracture replica labeling. *J Neurosci* 27: 2135-2144.
- Mauk, M.D., Garcia, K.S., Medina, J.F., and Steele, P.M. (1998). Does cerebellar LTD mediate motor learning? Toward a resolution without a smoking gun. *Neuron* 20: 359-362.
- Minke, B. (1977). Drosophila mutant with a transducer defect. *Biophysics of structure and mechanism* 3: 59-64.
- Miyata, M., Finch, E.A., Khiroug, L., Hashimoto, K., Hayasaka, S., Oda, S.I., Inouye, M., Takagishi, Y., Augustine, G.J., and Kano, M. (2000). Local calcium release in dendritic spines required for long-term synaptic depression. *Neuron* 28: 233-244.
- Miyata, M., Kim, H.T., Hashimoto, K., Lee, T.K., Cho, S.Y., Jiang, H., Wu, Y., Jun, K., Wu, D., Kano, M., and Shin, H.S. (2001). Deficient long-term synaptic depression in the rostral cerebellum correlated with impaired motor learning in phospholipase C beta4 mutant mice. *The European journal of neuroscience* 13: 1945-1954.
- Moepps, B., and Fagni, L. (2003). Mont Sainte-Odile: a sanctuary for GPCRs. Confidence on signal transduction of G-protein-coupled receptors. *EMBO reports* 4: 237-243.
- Montell, C., Birnbaumer, L., Flockerzi, V., Bindels, R.J., Bruford, E.A., Caterina, M.J., Clapham, D.E., Harteneck, C., Heller, S., Julius, D., *et al.* (2002). A unified nomenclature for the superfamily of TRP cation channels. *Molecular cell* 9: 229-231.
- Montell, C., Jones, K., Hafen, E., and Rubin, G. (1985). Rescue of the Drosophila phototransduction mutation *trp* by germline transformation. *Science* 230: 1040-1043.
- Nakamura, M., Sato, K., Fukaya, M., Araishi, K., Aiba, A., Kano, M., and Watanabe, M. (2004). Signaling complex formation of phospholipase Cbeta4 with metabotropic glutamate receptor type 1alpha and 1,4,5-trisphosphate receptor at the perisynapse and endoplasmic reticulum in the mouse brain. *The European journal of neuroscience* 20: 2929-2944.

- Nakanishi, S. (1992). Molecular diversity of glutamate receptors and implications for brain function. *Science* 258: 597-603.
- Nakao, H., Nakao, K., Kano, M., and Aiba, A. (2007). Metabotropic glutamate receptor subtype-1 is essential for motor coordination in the adult cerebellum. *Neuroscience research* 57: 538-543.
- Nicoletti, F., Iadarola, M.J., Wroblewski, J.T., and Costa, E. (1986a). Excitatory amino acid recognition sites coupled with inositol phospholipid metabolism: developmental changes and interaction with alpha 1-adrenoceptors. *Proceedings of the National Academy of Sciences of the United States of America* 83: 1931-1935.
- Nicoletti, F., Wroblewski, J.T., Novelli, A., Alho, H., Guidotti, A., and Costa, E. (1986b). The activation of inositol phospholipid metabolism as a signal-transducing system for excitatory amino acids in primary cultures of cerebellar granule cells. *J Neurosci* 6: 1905-1911.
- Nusser, Z., Mulvihill, E., Streit, P., and Somogyi, P. (1994). Subsynaptic segregation of metabotropic and ionotropic glutamate receptors as revealed by immunogold localization. *Neuroscience* 61: 421-427.
- Paredes, R.M., Etzler, J.C., Watts, L.T., Zheng, W., and Lechleiter, J.D. (2008). Chemical calcium indicators. *Methods (San Diego, Calif)* 46: 143-151.
- Piochon, C., Irinopoulou, T., Bruscianno, D., Bailly, Y., Mariani, J., and Levenes, C. (2007). NMDA receptor contribution to the climbing fiber response in the adult mouse Purkinje cell. *J Neurosci* 27: 10797-10809.
- Putney, J.W., Jr. (2004). The enigmatic TRPCs: multifunctional cation channels. *Trends in cell biology* 14: 282-286.
- Ramsey, I.S., Delling, M., and Clapham, D.E. (2006). An introduction to TRP channels. *Annual review of physiology* 68: 619-647.
- Renzi, M., Farrant, M., and Cull-Candy, S.G. (2007). Climbing-fibre activation of NMDA receptors in Purkinje cells of adult mice. *The Journal of physiology* 585: 91-101.
- Riccio, A., Li, Y., Moon, J., Kim, K.S., Smith, K.S., Rudolph, U., Gapon, S., Yao, G.L., Tsvetkov, E., Rodig, S.J., et al. (2009). Essential role for TRPC5 in amygdala function and fear-related behavior. *Cell* 137: 761-772.
- Salome, R., Kremer, Y., Dieudonne, S., Leger, J.F., Krichevsky, O., Wyart, C., Chatenay, D., and Bourdieu, L. (2006). Ultrafast random-access scanning in two-photon microscopy using acousto-optic deflectors. *Journal of neuroscience methods* 154: 161-174.

- Schmahmann, J.D. (2004). Disorders of the cerebellum: ataxia, dysmetria of thought, and the cerebellar cognitive affective syndrome. *The Journal of neuropsychiatry and clinical neurosciences* 16: 367-378.
- Shigemoto, R., Nakanishi, S., and Mizuno, N. (1992). Distribution of the mRNA for a metabotropic glutamate receptor (mGluR1) in the central nervous system: an in situ hybridization study in adult and developing rat. *J Comp Neurol* 322: 121-135.
- Shin, J.H., and Linden, D.J. (2005). An NMDA receptor/nitric oxide cascade is involved in cerebellar LTD but is not localized to the parallel fiber terminal. *Journal of neurophysiology* 94: 4281-4289.
- Sillevis Smitt, P., Kinoshita, A., De Leeuw, B., Moll, W., Coesmans, M., Jaarsma, D., Henzen-Logmans, S., Vecht, C., De Zeeuw, C., Sekiyama, N., et al. (2000). Paraneoplastic cerebellar ataxia due to autoantibodies against a glutamate receptor. *The New England journal of medicine* 342: 21-27.
- Sladeczek, F., Pin, J.P., Recasens, M., Bockaert, J., and Weiss, S. (1985). Glutamate stimulates inositol phosphate formation in striatal neurones. *Nature* 317: 717-719.
- Sugiyama, H., Ito, I., and Hirono, C. (1987). A new type of glutamate receptor linked to inositol phospholipid metabolism. *Nature* 325: 531-533.
- Sugiyama, T., Hirono, M., Suzuki, K., Nakamura, Y., Aiba, A., Nakamura, K., Nakao, K., Katsuki, M., and Yoshioka, T. (1999). Localization of phospholipase Cbeta isozymes in the mouse cerebellum. *Biochemical and biophysical research communications* 265: 473-478.
- Tai, Y., Feng, S., Du, W., and Wang, Y. (2009). Functional roles of TRPC channels in the developing brain. *Pflugers Arch* 458: 283-289.
- Takechi, H., Eilers, J., and Konnerth, A. (1998). A new class of synaptic response involving calcium release in dendritic spines. *Nature* 396: 757-760.
- Talavera, K., Nilius, B., and Voets, T. (2008). Neuronal TRP channels: thermometers, pathfinders and life-savers. *Trends in neurosciences* 31: 287-295.
- Tempia, F., Alojado, M.E., Strata, P., and Knopfel, T. (2001). Characterization of the mGluR(1)-mediated electrical and calcium signaling in Purkinje cells of mouse cerebellar slices. *Journal of neurophysiology* 86: 1389-1397.

- Tempia, F., Miniaci, M.C., Anchisi, D., and Strata, P. (1998). Postsynaptic current mediated by metabotropic glutamate receptors in cerebellar Purkinje cells. *Journal of neurophysiology* 80: 520-528.
- Tu, J.C., Xiao, B., Naisbitt, S., Yuan, J.P., Petralia, R.S., Brakeman, P., Doan, A., Aakalu, V.K., Lanahan, A.A., Sheng, M., and Worley, P.F. (1999). Coupling of mGluR/Homer and PSD-95 complexes by the Shank family of postsynaptic density proteins. *Neuron* 23: 583-592.
- Tu, J.C., Xiao, B., Yuan, J.P., Lanahan, A.A., Leoffert, K., Li, M., Linden, D.J., and Worley, P.F. (1998). Homer binds a novel proline-rich motif and links group 1 metabotropic glutamate receptors with IP3 receptors. *Neuron* 21: 717-726.
- Vannier, B., Zhu, X., Brown, D., and Birnbaumer, L. (1998). The membrane topology of human transient receptor potential 3 as inferred from glycosylation-scanning mutagenesis and epitope immunocytochemistry. *The Journal of biological chemistry* 273: 8675-8679.
- Venkatachalam, K., and Montell, C. (2007). TRP Channels. *Annual review of biochemistry* 76: 387-417.
- Villereal, M.L. (2006). Mechanism and functional significance of TRPC channel multimerization. *Seminars in cell & developmental biology* 17: 618-629.
- Wang, S.S., Denk, W., and Hausser, M. (2000). Coincidence detection in single dendritic spines mediated by calcium release. *Nature neuroscience* 3: 1266-1273.
- Wes, P.D., Chevesich, J., Jeromin, A., Rosenberg, C., Stetten, G., and Montell, C. (1995). TRPC1, a human homolog of a Drosophila store-operated channel. *Proceedings of the National Academy of Sciences of the United States of America* 92: 9652-9656.
- Worley, P.F., Zeng, W., Huang, G.N., Yuan, J.P., Kim, J.Y., Lee, M.G., and Muallem, S. (2007). TRPC channels as STIM1-regulated store-operated channels. *Cell Calcium* 42: 205-211.
- Yamakawa, Y., and Hirano, T. (1999). Contribution of mGluR1 to the basal activity of a mouse cerebellar Purkinje neuron. *Neuroscience letters* 277: 103-106.
- Yasuda, R., Nimchinsky, E.A., Scheuss, V., Pologruto, T.A., Oertner, T.G., Sabatini, B.L., and Svoboda, K. (2004). Imaging calcium concentration dynamics in small neuronal compartments. *Sci STKE* 2004: pl5.

- Yuan, Q., Qiu, D.L., Weber, J.T., Hansel, C., and Knopfel, T. (2007). Climbing fiber-triggered metabotropic slow potentials enhance dendritic calcium transients and simple spike firing in cerebellar Purkinje cells. *Mol Cell Neurosci*.
- Zhou, F.W., Matta, S.G., and Zhou, F.M. (2008). Constitutively active TRPC3 channels regulate basal ganglia output neurons. *J Neurosci* 28: 473-482.
- Zhu, X., Chu, P.B., Peyton, M., and Birnbaumer, L. (1995). Molecular cloning of a widely expressed human homologue for the *Drosophila* trp gene. *FEBS Lett* 373: 193-198.
- Zitt, C., Obukhov, A.G., Strubing, C., Zobel, A., Kalkbrenner, F., Luckhoff, A., and Schultz, G. (1997). Expression of TRPC3 in Chinese hamster ovary cells results in calcium-activated cation currents not related to store depletion. *The Journal of cell biology* 138: 1333-1341.
- Zufall, F. (2005). The TRPC2 ion channel and pheromone sensing in the accessory olfactory system. *Naunyn-Schmiedeberg's archives of pharmacology* 371: 245-250.